Marine and Petroleum Geology 89 (2018) 515–529

Contents lists available at ScienceDirect

Marine and Petroleum Geology

journal homepage: www.elsevier.com/locate/marpetgeo

Research paper

Multistage dolomitization in Late Jurassic–Early Cretaceous platform carbonates (Berdiga Formation), Başoba Yayla (Trabzon), NE Turkey: Implications of the generation of magmatic arc on dolomitization

M. Ziya Kırmacı[a], Merve Yıldız[a,*], Raif Kandemir[b], Tuğba Eroğlu-Gümrük[a]

[a] Department of Geological Engineering, Karadeniz Technical University, 61080, Trabzon, Turkey
[b] Department of Geological Engineering, Recep Tayyip Erdoğan University, 53100, Rize, Turkey

ARTICLE INFO

Keywords:
Dolomitization
Geochemistry
Recrystallization
Late Jurassic–Early cretaceous
Platform carbonates
Arc magmatism
Eastern pontides
NE Turkey

ABSTRACT

Late Jurassic–Early Cretaceous Berdiga Formation, which is widely distributed in an E-W trending belt in the Eastern Pontides (NE Turkey), is composed of platform carbonates. The formation shows varying lithofacies changing from supratidal to platform margin reef both laterally and vertically. The studied Başoba Yayla (Trabzon, NE Turkey) area comprises one of the typical exposures of formation in the northern zone of Eastern Pontides. In this area, the lower parts of the formation are pervasively dolomitized by fabric-destructive and fabric-preserving replacive dolomites that are Ca rich and nonstoichiometric ($Ca_{56-60}Mg_{40-44}$). Replacement dolomites (Rd) are represented by $\delta^{18}O$ values of −15.3 to −4.2 (VPDB), $\delta^{13}C$ values of −3.7–1.5‰ (VPDB), and $^{87}Sr/^{86}Sr$ ratios of 0.70675–0.70731. Petrographic and geochemical evidence implies that Rd dolomites are formed before compaction at shallow-moderate burial depths from Late Jurassic–Early Cretaceous seawater and/or partly modified seawater as a consequence of rock/water interaction, and they are recrystallized at elevated temperatures during subsequent burial. During subsequent Late Cretaceous diagenetic process when the region became a magmatic arc, Rd1a and Rd3 dolomite were recrystallized by hydrothermal fluids of marine origin. The dolomite cements (Cd) overlying the low-amplitude stylolites have similar geochemical charasteristics than Rd1a and Rd3 dolomite and are characterized by high homogenization temperatures (Th). This might indicate that Cd dolomite was precipitated from hydrothermal fluids of marine origin that recrystallized the Rd1a and Rd3 dolomite.

The fact that Cd dolomite comprising the latest phase of dolomitization is overlain by coarsely crystalline mosaic calcite and silica cements may indicate that diagenetic fluids were undersaturated with respect to dolomite and oversaturated with respect to calcite and silica.

1. Introduction

Dolomitization of platform carbonates is a common diagenetic process that is still not fully understood. Therefore, research on understanding dolomitizing processes has received tremendous attention. Although several dolomitization models (e.g. evaporative, back seepage, mixing zone, burial and seawater dolomitization models) are proposed that vary with respect to sedimentological and hydrological settings, the origin of massive dolomites is still controversial (Land, 1980, 1992; Morrow, 1982, 1998). Recrystallization and hydrothermal alteration of dolomites during burial diagenesis make difficult to assess their evolution due to modification of their primary texture as well as petrographic and geochemical characteristics. Among the proposed models, seawater dolomitization model is believed to be the most plausible model for dolomitization of platform carbonates (Vahrenkamp and Swart, 1990; Suzuki et al., 2006; Kırmacı, 2008). In recent studies, hydrothermal dolomitization and/or hydrothermal alteration have become a new understanding to dolomitization (Davies and Smith, 2006). Studies also revealed that hydrothermal dolomitization and/or hydrothermal alteration are more common than thought (e. g., Davies and Smith, 2006; Nader et al., 2009, 2012; Lo´pez-Horgue et al., 2010; Hong et al., 2016) and are generally related to tectono-magmatic activities (e. g., Cervato, 1990; Wilson et al., 1990; Dong et al., 2013; Shah et al., 2010).

Eastern Pontides (NE Turkey) in the Pontide mountain belt cover an area of 500 km in length and 100 km in width that extends from Kızılırmak or Yeşilırmak rivers in the vicinity of Samsun to the Lesser Caucasus along the southeastern coast of Black Sea (Fig. 1). This area

* Corresponding author.
E-mail addresses: kirmaci@ktu.edu.tr (M.Z. Kırmacı), merveyildiz@ktu.edu.tr (M. Yıldız).

http://dx.doi.org/10.1016/j.marpetgeo.2017.10.018
Received 4 May 2017; Received in revised form 17 October 2017; Accepted 20 October 2017
Available online 23 October 2017
0264-8172/ © 2017 Elsevier Ltd. All rights reserved.

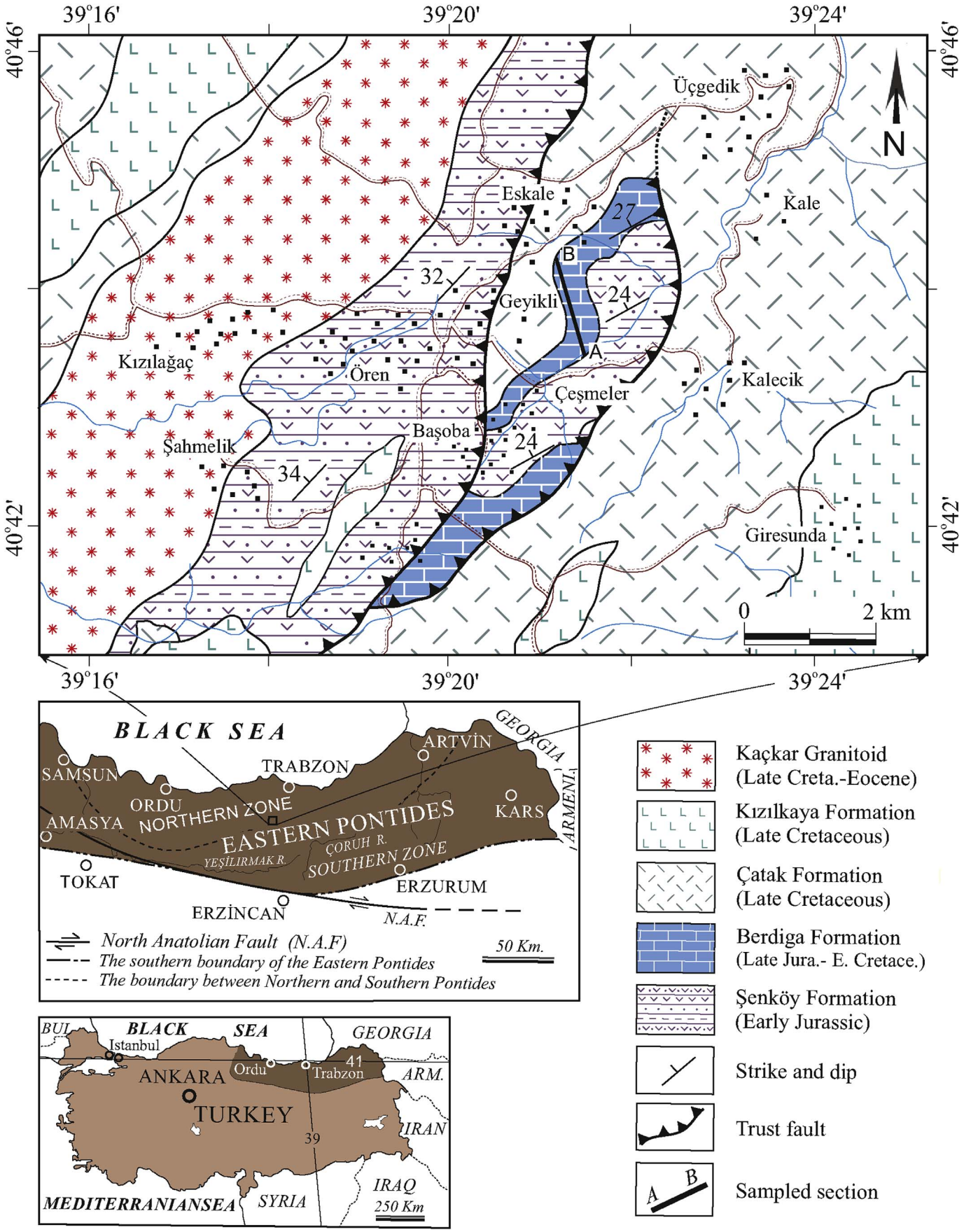

Fig. 1. Geological map and generalized stratigraphic columnar section of the Başoba Yayla area (Trabzon, NE Turkey)(modified after Güven, 1993).

which is represented by multi-phase tectonic and magmatic activities and experienced deformation during the Mesozoic time is a large and complex sedimentary basin and was filled by platform carbonates (Berdiga Formation) during the late Jurassic-early Cretaceous. Lower parts of these carbonates particularly the areas close to main faults that define the borders of early-middle Jurassic rift basin have been pervasively dolomitized (Kırmacı, 1992). Although biostratigraphic and lithofacies properties of platform carbonates have been studied (Kırmacı, 1992; Taslı, 1991; Kırmacı et al., 1996; Koch et al., 2008 and several others), there has been no study on dolomitization.

This study aims to investigate the mechanism of dolomitization in late Jurassic-early Cretaceous platform carbonates (Berdiga Formation) and determine the origin and geochemical nature of dolomitizing fluids in relation with tectono-magmatic events. For this reason, Başoba Yayla (Trabzon, NE Turkey) section (Fig. 1b) has been selected since in this area magmatic and tectonic events are often recognized and Eastern Pontide Northern Zone and dolomites are well exposed.

2. Geological setting

Pre-Jurassic basement rocks in the Eastern Pontides are composed of a pre-Carboniferous high-degree metamorphic complex and an early Carboniferous granodiorite-dacite complex (Okay and Şahintürk, 1997). In the northern zone of Eastern Pontides, the Mesozoic sedimentation starts with rift deposits consisting of volcanoclastic rocks (Early Jurassic Şenköy Formation) unconformably overlying the heterogeneous basement (Akın, 1979; Okay and Şahintürk, 1997; Yılmaz and Kandemir, 2006). The Şenköy Formation with a thickness of 2–2000 m shows lateral and vertical facies changes and is composed of volcanic sandstone, shale, conglomerate, basalt, andesite, and an alternation of their pyroclasts (Gedik et al., 1996; Okay and Şahintürk, 1997; Yılmaz and Kandemir, 2002). It also contains *Ammonitico-rosso* horizons and coal veins without lateral continuity (Boynukalın, 1990). The early Jurassic Şenköy Formation is conformably overlain by the Late Jurassic–Early Cretaceous Berdiga Formation consisting of platform carbonates. The Berdiga Formation with limited distribution in the northern zone of Eastern Pontides displays different lithofacies characteristics both laterally and vertically. The lithofacies evolution and fauna content of the formation are indicative of shelf environments changing from subratidal to fore reef (Pelin, 1977; Kırmacı, 1992; Kırmacı et al., 1996; Koch et al., 2008). In the study area, the lower part of the formation is completely dolomitized (Fig. 2) and the middle and upper parts are developed while dispaying grainstone-packstone and skeletal wackestone lithofacies features, respectively (Taslı et al., 1999).

Although platform carbonates in the southern zone of Eastern Pontides (Berdiga Formation) are confined to the main Senonian unconformity, which resulted in erosion of the whole carbonate sequence, there is no significant interruption between Lower and Upper Cretaceous in the northern zone (Okay and Şahintürk, 1997).

The Late Cretaceous volcano-sedimentary sequence (Akın, 1979; Okay and Şahintürk, 1997) with a thickness more than 2000 m that was deposited in rift basins reflects superficial sediments of the magmatic arc and is widely observed in the northern zone of the Eastern Pontides. The base of the volcano-sedimentary series comprises basalt, andesite, and their pyroclasts alternating with volcanic sandstone, clayey limestone, claystone, and claret red colored pelagic limestones (Çatak Formation); the middle levels are composed of dacite, rhyodacite, and their pyroclasts with clayey-sandy limestone interlayers (Kızılkaya Formation). These rocks change upward to volcanic sandstone that is interbedded with spilitic basalt and andesite, claystone, clayey limestone, and pelagic limestones (Çağlayan Formation) and rhyolite, rhyodacite, and their pyroclasts (Çayırbağ Formation). Maastrichtian-Danian limestone turbidites (Tonya Formation) formed the uppermost part of the sequence (Kırmacı and Akdağ, 2005). All these units are intruded by Late Cretaceous-Eocene granitic rocks (Kaçkar Granitoid) that are widely exposed in the region (Gedik et al., 1996; Güven, 1993; Kaygusuz et al., 2009). The Eocene rocks (Kabaköy Formation) that unconformably overlie the Late Cretaceous and older rocks are widely distributed in the northern zone of Eastern Pontides. The Eocene rocks that are the products of calc-alkaline type volcanism and shallow marine sedimentation are composed of marl and sandy limestone interbedded andesite, basalt, and their pyroclasts.

3. Methods

For this study, 100 samples with a spacing of 0.5–1.5 m were collected from Başoba Yayla area (Trabzon, NE Turkey), where Late Jurassic–Early Cretaceous platform carbonates of the northern zone of Eastern Pontides are well exposed (Figs. 1 and 2). Petrographic analysis was conducted on thin sections that were stained with alizerin-redS and potassium ferricyanide (Dickson, 1966). Cathodoluminescence characteristics of selected samples were performed at the Istanbul Technical University with CITL (Cambridge Image Technology Ltd.) Cold Cathodoluminescence, Model 8200 Mk5-2 mounted on a Nikon Eclipse LV100-POL microscope integrated with an optical spectrometer (OS) and an energy-dispersive spectrometer (EDX). The system was operated at 10–20 kV and 450–500 mA conditions, and a vacuum was fixed at 100–1000 mbar. X-ray diffractometry (XRD) of selected samples was done with a Rigaku DMAX IIC x-ray diffractometer (Cu-Kα radiation ~35 kV, 15 mA). Scanning rate was 2°/min with 5–70° 2θ. Microthermometric measurements of fluid inclusions were carried out with Linkam THMSG-600 with cooling/heating stage. Temperatures of homogenization and last ice melting have standard errors of ± 0.1 °C. Tm values were used to calculate salinity expressed as wt% NaCl equivalent (Bodnar, 1993): wt% NaCl = $1.78*T_m - 0{,}0442*(T_m)^2 + 0{,}000557*(T_m)^3$ (Bodnar, 1993).

Major (Ca, Mg) and trace (Na, Mn, Fe, and Sr) element contents of selected 28 dolomite and 3 belemnite samples were determined with the ICP-EAS (Inductively Coupled Plasma-Atomic Emission Spectrometer) method. Sample preparation (dissolving in acid and filtering) and measurements were conducted at ACME Analytical Laboratories Ltd. (Canada). Major oxide compositions were determined by ICP-ES from pulps after 0.2 g samples of rock powder were fused with 1.5 g LiBO2 and then dissolved in 100 ml 5% HNO3. Trace and rare earth element contents were analyzed by ICP-MS from pulps after 0.2 g samples of rock powder were dissolved by four acid digestions. Dedection limit of elements is 0.01% for Ca, Mg, Na, and Fe and 5 ppm for Mn and Sr.

The same dolomite and belemnite samples (10–15 mg) were also analyzed for their oxygen and carbon isotope contents. These analyses ($\delta^{18}O$ and $\delta^{13}C$) were conducted at the Pacific Centre for Isotopic and Geochemical Research (PCIGR) laboratories of the Bristol Columbia University. Analyses were carried out using the gas bench and a Delta Plus XL mass spectrometer in continuous flow mode. The $\delta^{13}C$ (VPDB) and d ^{18}O (VSMOW) column are results corrected to VPBD and VSMOW based on an average of multiple analyses of NBS stds 18 & 19. Samples were acidified with 99% Phosphoric Acid in helium-flushed sealed vials, and the headspace gas was measured in a helium flow. $^{87}Sr/^{86}Sr$ isotope ratios of these samples were also measured at the same laboratory. Concentrations were measured at Thermo Finnigan Element II, High-Resolution ICP-MS by using the method described by Pretorius et al. (2006).

4. Results

4.1. Dolomite petrography

In the studied section, lower part of the studied section is pervasively dolomitized by replacive (Rd) and cement (Cd) type dolomites (Fig. 3). Based on petrographic properties such as crystal boundary, shape, and crystal size (planar and/or non-planar; Sibley and Gregg,

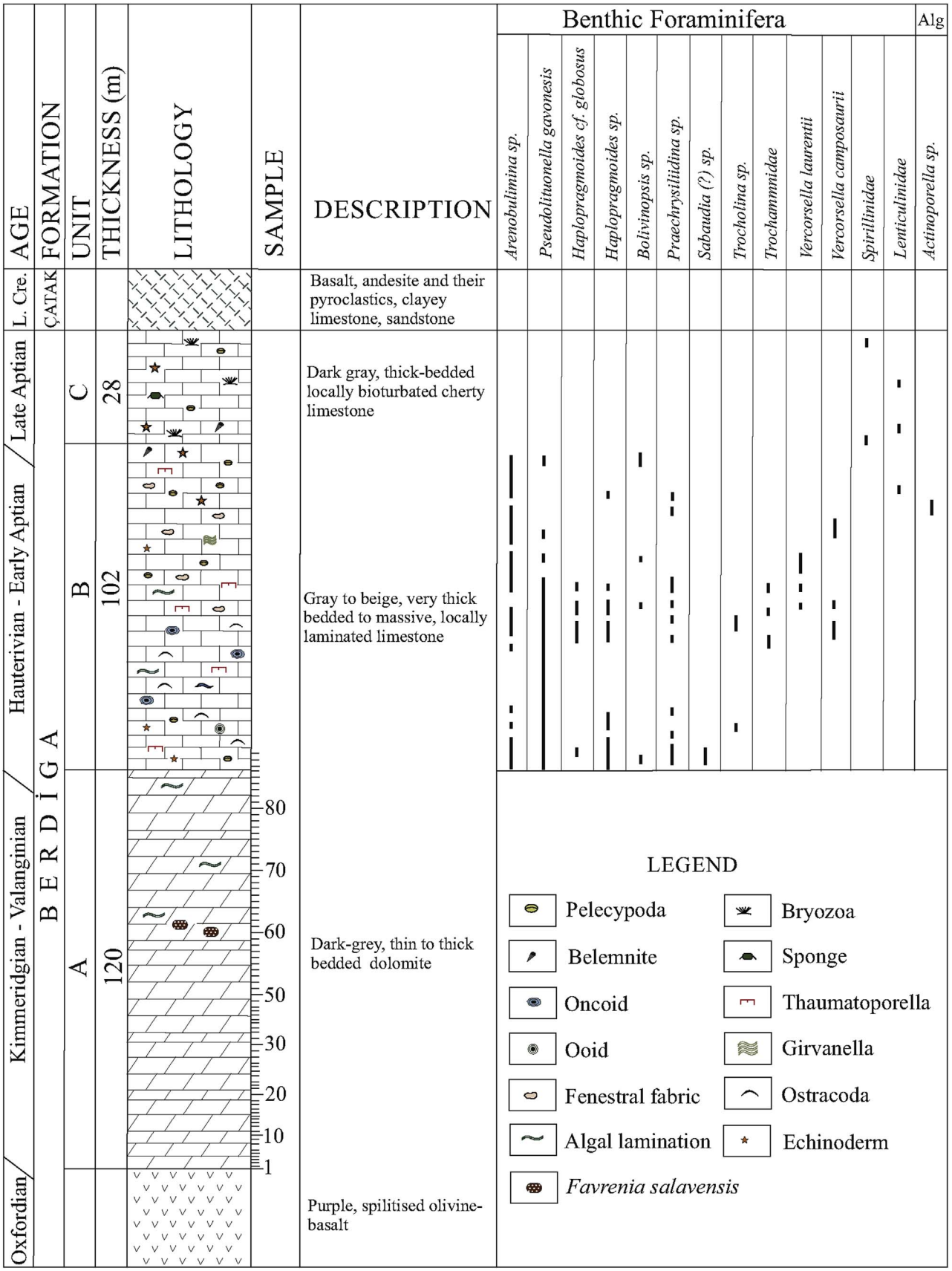

Fig. 2. Columnar section showing lithofacies characteristics and stratigraphic distributions of benthic foraminiferas, algae and dolomite types ofBerdiga Formation.

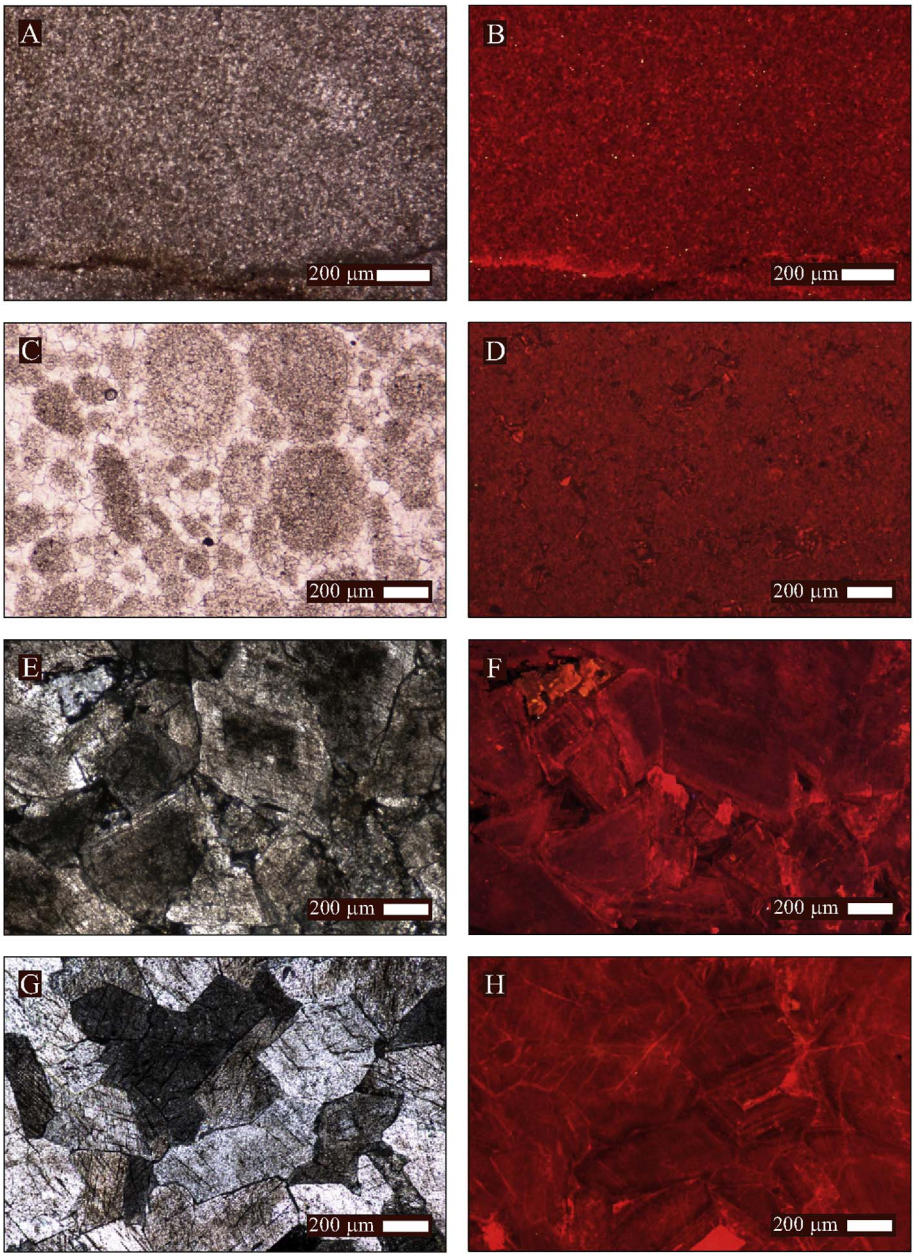

Fig. 3. Paired cross-polarized and cathodoluminescent photomicrographs showing the replacement dolomites (Rd1, Rd2 and Rd3) and dolomite cement (Cd) observed at the Berdiga Formation.

1987), four types of dolomite were described (Fig. 3).

4.1.1. Replacement dolomites (Rd)

4.1.1.1. Fine crystalline planar-s dolomite (Rd1). Rd1 dolomite has an abundance of about 20–25% (volumetrically), and it replaces very thin-layered (3–15 cm) muddy facies (particularly mudstones). The presence of fenestral porosity in layers replaced by Rd1 dolomite might indicate that they were deposited in a supratidal environment or in the upper part of intertidal environments. Rd1 dolomite consists of 5–30 µm (rarely up to 50 µm) crystals with planar-s (with slight nonplanar-a) fabric (Fig. 3A). Under cathodoluminescence (CL), Rd1 dolomite is generally orange-dull reddish colored (Fig. 3B). Although Rd1 dolomite petrographically has a uniform fabric, geochemically it shows bimodal distribution (Fig. 4; Table 1). Therefore Rd1 dolomite is subdivided into two subtypes. Based on this, fractured and/or brecciated Rd1 dolomite at the lower part of the dolomite sequence that forms the first population is defined as Rd1a, whereas Rd1 dolomite at the upper part of the dolomite sequence that comprises the second population is defined as Rd1b.

4.2. Fabric-preserving, fine–medium crystalline planar-s dolomite (Rd2)

Rd2 dolomite is fabric preserving, and it occurs only in peloidal grainstone and packstone facies that are thin–medium bedded (about 10–30 cm). It comprises about 10–15% (by volume) of all dolomitized phases. Rd2 dolomite comprises 20–100 µm (40–60 µm on average) crystals with planar-s texture that exhibit a sharp extinction (Fig. 3C). Under CL, Rd2 dolomite has a reddish to nonluminescence appearance (Fig. 3D). Rd2 dolomite is characterized by poor intercrystalline porosity, because its planar-s crystal is tightly interlocked.

4.3. Coarse–very coarse crystalline planar-s dolomite (Rd3)

RD3 dolomite has a fabric-destructive character. Rd3 dolomite is the most common dolomite type in the Berdiga Formation, and it consists of about 60–65% of the whole dolomite phase replacing limestones of all facies except for muddy facies. Rd3 dolomite has a planar-s and rarely nonplanar texture, and it comprises crystals that are 400 µm–1.2 mm (mostly 500–600 µm) in size (Fig. 3E). Under CL, Rd3 dolomite shows

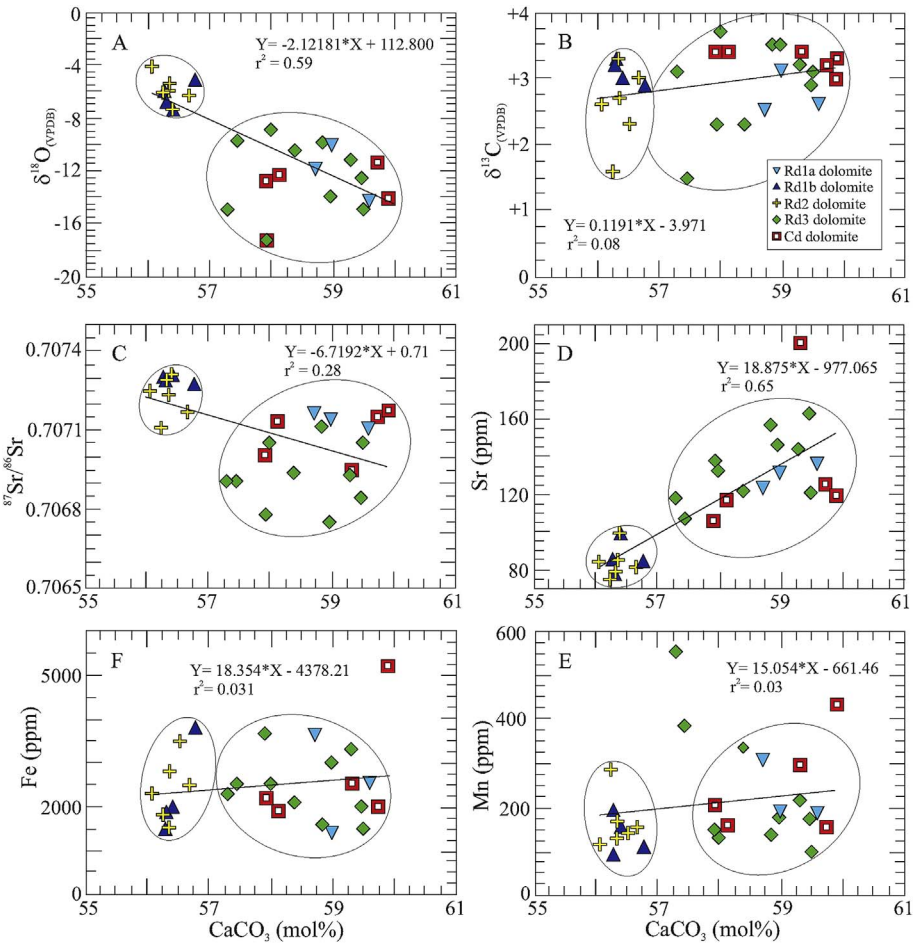

Fig. 4. Cross-plots of $\delta^{18}O$,$\delta^{13}C$,$^{87}Sr/^{86}Sr$,Sr, Fe andMnvalues versus $CaCO_3$ with calculated regression axis of the replacement dolomites (Rd1a, Rd1b, Rd2 and Rd3) and dolomite cement (Cd) from Berdiga Formation.

purplish and/or dull red color (Fig. 3F). Rd3 dolomite generally has a low intergranular porosity, since crystals are tightly interlocked.

4.3.1. Dolomite cement (Cd)

Dolomite cement (Cd) appears to either completely or partially fill vuggy/molds and fractures in Rd1 dolomites. Pores are filled by not only Cd dolomite cement but also late-phase cements such as mosaic calcite and/or megaquartz. Volumetrically, Cd comprise accounting for only 2–5% of the entire dolomite phase. Cd comprises planar crystals with a size in the range of 0.4–1.2 mm that exhibit a sharp extinction (Fig. 3G). Under CL, Cd shows none to dull orange-red luminescence (Fig. 3H).

4.4. Dolomite geochemistry

Results of $\delta^{13}C$, $\delta^{18}O$, and $^{87}Sr/^{86}Sr$ isotope and trace element analyses of dolomites from the studied section and of three belemnite samples collected from limestones just above the dolomite sequence in the vicinity of study area are given in Fig. 4 and Table 1. Although Rd1 dolomite petrographically has a uniform fabric, geochemically it shows bimodal distribution (Fig. 4; Table 1).

4.4.1. Major and trace elements

In the studied section, dolomites of Berdiga Formation are non-stoichiometric and have a total of 56.1–59.9 mol% $CaCO_3$ (average 58.0 mol%; n = 28) and 40.1–43.9 mol% $MgCO_3$ (average 42.0 mol%; n = 28) contents. Chemical analyses of dolomite samples containing Rd1a, Rd1b, Rd2 and Rd3 and Cd are presented in Table 1. Based on this, dolomites of the Berdiga Formation are significantly depleted in Na and Sr with respect to belemnite samples but they are notably enriched in Fe and Mn (Table 1). Trace element contents of replacement dolomites do not show any variation with depth (Fig. 5).

4.4.2. Oxygen and carbon isotopes

Although dolomites of Berdiga Formation are represented by variable depleted $\delta^{18}O$ values (−17.3‰ to −4.1‰ VPDB), their $\delta^{13}C$ values are very close (1.5‰–3.7‰ VPDB) (Fig. 6A and B; Table 1). $\delta^{18}O$ values of Rd1a and Rd1b are −14.3‰ to −10.1‰ VPDB (average −12.1‰ VPDB; n = 3) and −7.4‰ to −5.1‰ VPDB (average −6.3‰ VPDB; n = 4), and $\delta^{13}C$ values are 2.5‰–3.1‰ VPDB (average 2.8‰ VPDB, n = 3) and 2.9‰–3.3‰ VPDB (average 3.1‰ VPDB, n = 4), respectively. The $\delta^{18}O$ and $\delta^{13}C$ values of RD2 dolomite range from −6.3‰ to −4.1‰ VPDB (average −5.7‰ VPDB, n = 6) and from 1.6‰ to 3.3‰ VPDB (average 2.6‰ VPDB, n = 6), respectively. The $\delta^{18}O$ values of Rd3 are between −17.3‰ and −8.9‰ VPDB (average −14.4‰ VPDB, n = 10), and $\delta^{13}C$ values are between 1.5‰ and 3.7‰ VPDB (average 2.9‰ VPDB, n = 10). Cd dolomite is represented by $\delta^{18}O$ and $\delta^{13}C$ values of −14.1‰ to −11.4‰ VPDB (average −12.5‰ VPDB, n = 5) and 3.2‰–3.4‰ VPDB (average 3.3‰ VPDB, n = 5), respectively. $\delta^{18}O$ and $\delta^{13}C$ values of belemnite samples are −3.5‰ to −1.4‰ VPDB (average −2.4‰ VPDB, n = 3) and 0.1‰–1.0‰ VPDB (average 0.6‰ VPDB, n = 3).

4.4.3. Strontium isotopes

$^{87}Sr/^{86}Sr$ ratios of dolomites are in the range of 0.70730 to 0.70675 (Figs. 6C and 7; Table 1). $^{87}Sr/^{86}Sr$ ratios of Rd1a, Rd1b, Rd2, Rd3, and Cd dolomites are 0.70713–0.70716 (average 0.70723, n = 3), 0.707258–0.70730 (average 0.70728, n = 4), 0.70711–0.70729 (average 0.70721, n = 6), 0.70675–0.70711 (average 0.70693, n = 10), and 0.70694–0.70717 (average 0.707083, n = 5),

Table 1
Summary of geochemical data obtained from replacement dolomites (Rd1a, Rd1b, Rd2 and Rd3), dolomite cement and belemnites observed from the Berdiga Formation.

Dolomite Type			$CaCO_3$	$MgCO_3$	Na	Mn	Fe	Sr	$\delta^{13}C$	$\delta^{18}O$	$^{87}Sr/^{86}Sr$ (± 2σ)
			(mole %)	(mole %)	(ppm)	(ppm)	(ppm)	(ppm)	(‰ VPDB)	(‰ VPDB)	
Rd1	Rd1a	*n*	3	3	3	3	3	3	3	3	3
		S.D.	0.5	0.5		70	100	7	0.3	2.1	0.0
		Max.	59.6	41.3	bdl	307	3600	136	3.1	-10.1	0.707161 ± 08
		Min.	58.7	40.4	bdl	184	1400	123	2.5	-14.3	0.707103 ± 07
		Mean	59.2	40.9	bdl	227	2500	130	2.7	-12.1	0.707134 ± 08
	Rd1b	*n*	4	4	4	4	4	4	4	4	4
		S.D.	0.2	0.2	50	46	1023	8.7	0.2	1.0	0.0
		Max.	56.8	43.7	200	195	3800	99	3.3	-5.1	0.707315 ± 08
		Min.	56.3	43.2	100	94	1500	78	2.9	-7.4	0.707277 ± 08
		Mean	56.5	43.6	125	139	2300	87	3.1	-6.3	0.707298 ± 08
Rd2	s	*n*	6	6	6	6	6	6	6	6	6
		S.D.	0.2	0.2	54.7	61.8	715.5	4.7	0.6	0.8	0.0
		Max.	57.7	43.9	200	270	3500	87	3.3	-4.1	0.707295 ± 09
		Min.	56.1	42.3	100	118	1500	74	1.6	-6.3	0.707112 ± 07
		Mean	56.6	43.4	150	164	2416	80	2.6	-5.7	0.707226 ± 08
Rd3		*n*	10	10	10	10	10	10	10	10	10
		S.D.	0.8	0.8		142	693	18	0.7	2.8	0.0
		Max.	59.5	42.7	200	553	3600	163	3.7	-8.9	0.707114 ± 07
		Min.	57.3	40.5	bdl	99	1500	107	1.5	-17.3	0.706780 ± 08
		Mean	58.5	41.5		232	2440	135	2.9	-12.4	0.706928 ± 08
Cd		*n*	5	5	5	5	5	5	5	5	5
		S.D.	1	1		118	1383		0.1	1.1	0.0
		Max.	59.9	42.1	bdl	435	5200	201	3.4	-11.4	0.707177 ± 08
		Min.	57.9	40.1	bdl	154	1900	106	3.2	-14.1	0.706948 ± 08
		Mean	59.0	41.0	bdl	250	2760	134	3.3	-12.4	0.707083 ± 08
BLM		*n*	3	3	3	3	3	3	3	3	3
		S.D.	0.1	0.1	58	4		111	0.5	1.1	0.0
		Max.	98.9	1.2	800	15	bdl	1251	1.0	-3.5	0.707426 ± 08
		Min.	98.8	1.1	600	8	bdl	1038	0.1	-1.4	0.707414 ± 08
		Mean	98.9	1.2	700	12	bdl	1127	0.6	-2.4	0.707412 ± 08

respectively. $^{87}Sr/^{86}Sr$ ratios of belemnite samples are between 0.70739 and 0.70742 (average 0.707412, n = 3).

4.5. Fluid inclusions

Rd1 and Rd2 dolomite crystals are very small in size, and, therefore, they are excluded from fluid inclusion studies. Two-phase secondary fluid inclusionsare formed along annealed fractures of Rd3 and Cd dolomite crystals. Rd3 and Cd dolomites have two-phase primary fluid inclusions, and measurable inclusions are found only in rims of very large crystals. Primary fluid inclusions are irregular shaped with a width of 3–7 μm and a length of 5–12 μm. The vapor phase contains about 10–15% of inclusion volume. Because the size of primary fluid inclusions in Rd3 dolomite is very small, their last ice melting temperatures (T_m) could not be measured and, thus, the salinity of liquids forming them could not be calculated. Homogenization temperatures (T_h) of fluid inclusions in Rd3 dolomite, measured on four samples, range from 170 to 210 °C (average 190 °C, n = 12). Homogenization temperatures (T_h) and melting temperature values (T_m) of fluid inclusions of Cd dolomite, measured on three samples, were measured to be 168–185 °C (average 174 °C, n = 14) and −12.4 to −10 °C (average −11.2 °C, n = 4), respectively. Ice melting temperatures (T_m) were used to calculate fluid salinites of 13.9–16.3 wt% eq. wt%NaCl.

5. Discussion

5.1. Interpretation of the dolomitization history

5.1.1. Dolomite stoichiometry

In the studied section, dolomites of Berdiga Formation are represented by the total $CaCO_3$ content of 56.1–59.9 mol% (average 58.0 mol% $CaCO_3$) and these are nonstoichiometric (Table 1). Although mol% $CaCO_3$ contents of dolomites are very close, they show bimodal distribution in composition. Rd1b and Rd2 dolomites (56.1–57.7 mol% $CaCO_3$) of the first population have lower $CaCO_3$ content in comparison to Rd1a, Rd3, and Cd dolomites (57.3–59.9 mol% $CaCO_3$) of the second population (Table 1). The bimodal stoichiometry of dolomites occurs as a result of diagenetic evolution, because Ca-rich dolomites are generally more sensitive to diagenetic alteration than stoichiometric dolomites (Sibley et al., 1994; Chai and Navrotsky, 1995; Zhao and Jones, 2012a).

As summarized by Zhao and Jones (2012a, b), the dolomite stoichiometry is related to various factors such as: (1) Mg/Ca ratios of dolomitizing fluids, (2) water/rock ratio (close or open diagenetic system), (3) Mg source, and (4) time of interaction with dolomitizing fluids (Vahrenkamp and Swart, 1990; Budd, 1997; Zhao and Jones, 2012a, 2012b). Kaczmarek and Sibley (2011) suggested that dolomite stoichiometry reflects the Mg/Ca ratios of dolomitizing fluids, and high Mg/Ca ratios of dolomitizing fluids end up in much shorter induction periods (the time when dolomite first appears) and in much faster dolomitizing ratios; however, fluids with low Mg/Ca ratios give rise to longer induction periods and much slower dolomitizing ratios. Thus, solutions with low Mg/Ca ratios form Ca-rich dolomites whereas those with high ratios produce Mg-rich dolomites. Considering these relations

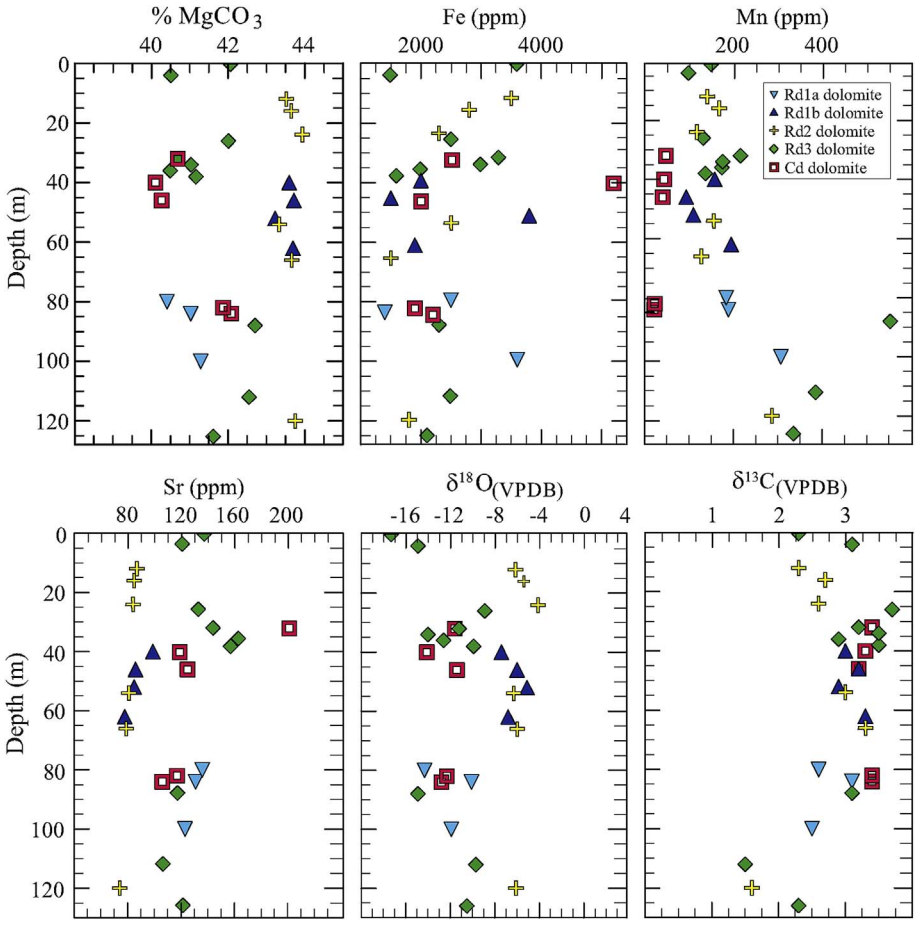

Fig. 5. Cross-plots showing stratigraphic variability in Fe, Mn, Sr, $\delta^{18}O$ and $\delta^{13}C$ values versus $MgCO_3$ of the replacement dolomites (Rd1a, Rd1b,Rd2 and Rd3) and dolomite cement (Cd) fromBerdiga Formation.

stated by Kaczmarek and Sibley (2011), it can be said that dolomitizing fluids that led to formation of bimodal Ca-rich dolomites (56.1–59.9 mol% $CaCO_3$) of Berdiga Formation have low Mg/Ca ratios and relatively slow dolomitizing rates. Similar to Cd dolomite, Rd1a and Rd3 dolomites are represented by $CaCO_3$ contents that are much higher than Rd1b and Rd2 dolomites. Differing from the case of Rd1b and Rd2 dolomites, this is explained by recrystallization of Rd1a and Rd3 dolomites by fluids with a high $CaCO_3$ content that also precipitated Cd dolomite.

Alteration of volcano-sedimentary rocks and mafic volcanic of Early–Middle Jurassic Şenköy Formation, which is conformably overlain by dolomites of Berdiga Formation, by Middle-Late Jurassic sea water origin resulted in spilitization of these rocks and extensive albitization of plagioclase (Şen, 2007). Therefore, the sea water which becomes Na-depleted whereas Ca-enriched due to this interaction, might be source of the dolomitizing fluids. The dolomitiziting fluid is heated by magmatic intrusions so the fluids are referred as hydrothermal waters of a sea water origin. Consequently, Ca-rich hydrothermal waters of a sea water origin migrated upward into dolomites and preferentially recrystallized Rd1a and Rd3 dolomites, making them more Ca enriched. The $CaCO_3$ content of Cd dolomite is within the range of Rd1a and Rd3 dolomite. This suggests that Cd was precipitated from fluids that recrystallized Rd1a and Rd3 dolomite. The filling of pore spaces that are left over from dolomite cement by mosaic calcite cement may imply that hydrothermal solutions have become undersaturated with respect to dolomite but oversaturated with calcite.

5.1.2. Oxygen and carbon isotopes

$\delta^{18}O$ values of dolomites are affected by various factors such as isotopic composition of dolomitizing fluids, temperature, kinetics (e.g. deposition rate, differentiation of phosphoric acid), and dolomite stoichiometry (Vahrenkamp and Swart, 1990; Budd, 1997; Zhao and Jones, 2012a, b); this makes it difficult to evaluate the resulting oxygen isotopic composition of dolomites. $\delta^{18}O$ values of dolomites reflect formation temperature and isotopic composition of dolomitizing fluids. In the study area, bimodal distribution of $\delta^{18}O$ values of replacement dolomites (Fig. 5A) in the Berdiga Formation might imply that they were formed by dolomitizing fluids with two discrete compositions and/or they were recrystallized.

Similar to other studies (e.g., Dawans and Swart, 1988; Vahrenkamp and Swart, 1990; Gill et al., 1995; Wheler et al., 1999; Suzuki et al., 2006a,b; Zhao and Jones, 2012a, b), there is a negative covariance between $\delta^{18}O$ and mol% Ca values of Berdiga dolomites (Fig. 4A). Previous studies show that $\delta^{18}O$ values are decreased by about 0.1–0.36‰ for each mol% Ca increase (Dawans and Swart, 1988; Vahrenkamp and Swart, 1990; Gill et al., 1995; Wheler et al., 1999; Suzuki et al., 2006a,b; Zhao and Jones, 2012a), but the decrease in $\delta^{18}O$ values of Berdiga dolomite is as much as 2.1‰. This correlation could be derived from some thermodynamic factors such as water temperature, dolomite stoichiometry, and isotopic composition of dolomitizing fluids (Land, 1980; Aharon et al., 1987; Wheler et al., 1999; Suzuki et al., 2006a,b) and some kinetic factors such as phosphoric acid fractionation and dolomitization rate (Aharon et al., 1977; Vahrenkamp and Swart, 1990; Zhao and Jones, 2012a). Phosphoric acid fractionation and dolomite stoichiometry result in a decrease in $\delta^{18}O$ of about 0.02‰ and 0.03–0.08‰, respectively, for each mol% Ca increase (Land, 1980; Aharon et al., 1987; Wheler et al., 1999). The change in $\delta^{18}O$ for one mol% Ca increase in each population for $\delta^{18}O$ values of bimodal Berdiga Rd dolomites is greater (0.23–0.88‰) than the range given earlier. In addition to this, considering $\delta^{13}C$ values of three belemnite samples from the Berdiga Formation ranging from +0.1 to +1.0‰ VPDB (average 0.6‰ VPDB) (Fig. 6A; Table 1), $\delta^{13}C$ values of

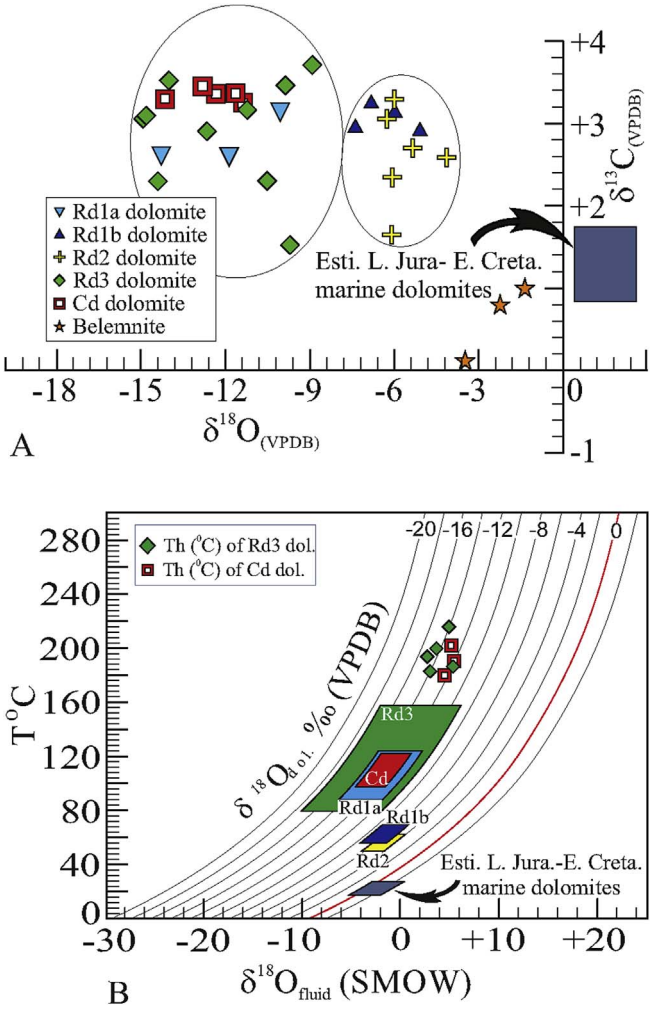

Fig. 6. (A) Oxygen and carbon isotopic compositions for replacement dolomites (Rd1a, Rd1b,Rd2and Rd3), dolomite cement (Cd) and belemnites. (B) Relationship between $\delta^{18}O$ of dolomite, $\delta^{18}O$ of water, and temperature, according to $10^3 \ln\alpha = 3.2*10^6\ T^{-2}$-3.3 (Sheppard and Schwarz, 1970). See text for explanations.

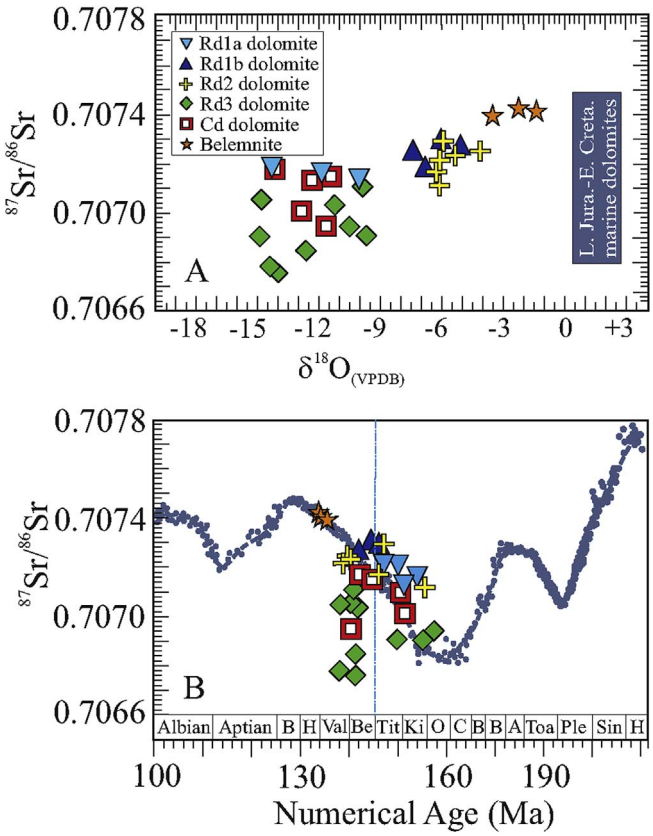

Fig. 7. A) Cross-plot of $\delta^{18}O$ values versus $^{87}Sr/^{86}Sr$ for replacement dolomites (Rd1a, Rd1bRd2 and Rd3),dolomite cement (Cd) and belemnites. B) $^{87}Sr/^{86}Sr$ values versus numerical age for the replacement dolomites (Rd1a, Rd1b Rd2 and Rd3),dolomite cement (Cd) and belemnites. Shown is the $^{87}Sr/^{86}Sr$ curve for the sea water during the Jurassic-Early Cretaceous time (after McArthur and Howarth, 2004).

dolomite deposited from the Late Jurassic–Early Cretaceous seawater should be about between +0.6 and + 2.0‰ VPDB (Fig. 6A). $\delta^{13}C$ values of replacement dolomites varying from +1.5 to +3.7‰ VPDB (average + 2.6‰ VPDB, n = 23) are conformable with those of dolomite precipitated from seawater (Fig. 6A). In addition, a diagenesis driven by meteoric waters under nomal conditions ends up in the formation of carbonates that have negative $\delta^{13}C$ values (Shields et al., 2003; Swart et al., 2005; Zhao and Jones, 2012a; Azomani et al., 2013). Positive $\delta^{13}C$ values and depleted $\delta^{18}O$ values of replacement dolomites might imply that they were recrystallized in a closed system and there was no meteoric water input before dolomitization. Recrystallization of dolomites in a closed system resets not $\delta^{13}C$ values but $\delta^{18}O$ values, and, therefore, dolomites may still retain carbon signals of marine deposits (Swart et al., 2005). $\delta^{18}O$ values of Rd1a and RD3 dolomites are noticeably depleted in comparison to those of Rd1b and Rd2 dolomites (Fig. 6). This happens as a result of preferential recrystallization of Rd1a and Rd3 dolomites by hydrothermal waters of a sea water origin during the Late Cretaceous era after their recrystallization in a closed system. Cd dolomite has $\delta^{18}O$ and $\delta^{13}C$ values that are similar to Rd1a and Rd3 dolomites (average + 3.3‰ VPDB) (Fig. 6A).

Considering that $\delta^{18}O$ values of −3.5 to −1.4‰ VPDB (average −2.4‰ VPDB) of three belemnite samples from the Berdiga Formation reflect temperature and isotopic equilibrium conditions of circulating seawater, calcite paleotemperature values might be predicted by using the equations of (1) Anderson and Arthur (1983): $T(°C) = 16.0–4.14*(\delta_{calcite} - \delta_{water}) + 0.13*(\delta_{calcite} - \delta_{water})^2$. The $\delta^{18}O$ value of seawater for the Late Jurassic–Early Cretaceous era can be assumed to be −1‰ VSMOW, which is characteristic for non-glacial periods on the Earth (Shackleton and Kennett, 1975). Consequently, paleotemperatures from both the equations are calculated in the range of 16.7–27.4 °C.

For this temperature interval, the $\delta^{18}O$ value of dolomite precipitating from Late Jurassic–Early Cretaceous ocean water (−1‰ VSMOW) is found to be 0.34–2.44‰ VPDB from the fractionation equation of $\Delta^{18}O$ ($\delta^{18}O_{dolomite} - \delta^{18}O_{calcite\text{-}belemnite}$) = 3.84‰ VPDB (e.g., Swart and Melim, 2000; MacNeil and Johns, 2003; Suzuki et al., 2006a,b).

At these temperatures, $\delta^{18}O$ values of Berdiga dolomites are much more negative than those precipitating from Late Jurassic–Early Cretaceous ocean water (Fig. 6). Depletion in $\delta^{18}O$ values of dolomites might be due to meteoric water input during the dolomitization (e.g. Gao et al., 1992; Smith and Dorobek, 1993; James et al., 1993; Mresah, 1998), elevated temperatures during recrystallization, and/or dolomitization during subsequent burial (Meyers et al., 1997; Mountjoy et al., 1999; Al-Aasm and Packard, 2000; Kırmacı and Akdağ, 2005; Swart et al., 2005; Kırmacı, 2008; etc). It is suggested that recent and old mixing zones cannot form pervasive dolomite sequences but can form only small-volume dolomites in the form of cement rather than replacement dolomite (Machel and Mountjoy, 1986; Hardie, 1987; Coniglio et al., 1988). In addition, positive $\delta^{13}C$ values of dolomites may indicate that before dolomitization limestones were not subjected to a meteoric diagenesis (Allan and Mathews, 1982; James and Choquette, 1990). Both these postulations reveal that meteoric waters did not significantly contribute to depletion of $\delta^{18}O$ values of

replacement dolomites of the Berdiga Formation.

As will be explained afterward, because of the early diagenetic origin of microcrystalline Rd1 and fabric-preserving Rd2 dolomites, $\delta^{18}O$ values of these dolomites will be determined from the oxygen isotope composition of pore waters (resembling $\delta^{18}O$ of Late Jurassic–Early Cretaceous seawater) and by their temperatures. In addition, it is also believed that unless early diagenetic dolomites are recrystallized at high temperatures, they cannot have higly depleted $\delta^{18}O$ values (Malone et al., 1996). Therefore, $\delta^{18}O$ values of Rd1 and Rd2 dolomites are probably depleted as a result of subsequent burial and recrystallization at elevated temperatures. $\delta^{18}O$ values of Rd1a dolomite are conformable with those of Rd3 and Cd dolomites, which are considerably depleted in comparison to $\delta^{18}O$ values of Rd1b and Rd2 dolomites (Fig. 6; Table 1). This indicates that both Rd1a and Rd3 dolomite, as distinct from Rd1 and Rd2 dolomite, were recrystallized by fluids from which the Cd dolomite was also precipitated.

$\delta^{18}O$ values of Cd dolomite are consistent with those of Rd1a and Rd3 dolomite (Fig. 6; Table 1). However, contrary to Rd1a and Rd3 dolomite, Cd dolomite overprints the low-amplitude stylolites, indicating that the formation of Cd dolomite postdates the stylolites. Taking into account the burial history of Berdiga Formation, low-amplitude stylolites that started to form at a burial depth of 500 m (Dunnington, 1967; Lind, 1993) were developed in the Late Cretaceous era when the region became a magmatic arc (Okay and Şahintürk, 1997) (Fig. 8). A minimum homogenization temperature of 168 °C (T_h) measured on Cd dolomite crystals requires that this dolomite is formed at minimum burial depths of 3.0–3.5 km, considering a surface temperature of 16.7–27.4 °C and under a maximum geothermic gradient of 45 °C km^{-1}. However, the burial history of Berdiga Formation is not consistent with such a burial depth (Fig. 8). This might show that Cd dolomite was deposited concurrently with hydrothermal fluids that recrystallized Rd1 and Rd3 dolomite.

5.1.3. Strontium isotopes

During carbonate deposition, isotopic fractionation factor of Sr becomes unimportant; hence, it is accepted that isotopic composition of marine carbonates reflects isotopic composition of seawater during the deposition (Veizer, 1983; Banner and Kaufman, 1994). Analyses on the marine carbonates show that $^{87}Sr/^{86}Sr$ ratios of oceans changed systematically during the Phanerozoic period but remained notably unchanged for open oceans of any period (Burke et al., 1982; Qing, 1998).

$^{87}Sr/^{86}Sr$ ratios of three belemnite samples from the Berdiga Formation are between 0.70739 and 0.70741 (average 0.70741) (Fig. 7; Table 1). When compared with the $^{87}Sr/^{86}Sr$ isotope curve of seawater (McArthur and Howarth, 2004), these values are found to correspond to $^{87}Sr/^{86}Sr$ values of limestone layers of the Valanginian-Houterivian time interval (Fig. 7B). This finding is also consistent with micropaleontological dating carried out on the same rocks (Taslı et al., 1999). Except for 2 samples of Rd3 dolomite, $^{87}Sr/^{86}Sr$ values of dolomites of the Berdiga Formation correspond with $^{87}Sr/^{86}Sr$ ratios of the Late Jurassic–Early Cretaceous (0.70680–0.70780; McArthur and Howarth, 2004) (Fig. 7B), indicating that these dolomites were deposited from waters that were similar to those of the Late Jurassic–Early Cretaceous period. In addition, $^{87}Sr/^{86}Sr$ ratios of Rd1a and Rd3 dolomite are lower than those of Rd1b and Rd2 dolomite (Fig. 7; Table 1), which may indicate that Rd1a and Rd3 dolomites were recrystallized by hydrothermal fluids of a sea water origin. Alteration of mafic volcanic rocks of Early Jurassic Şenköy Formation, which are conformably overlain by dolomites of the Berdiga Formation, by hydrothermal fluids of a marin origin resulted in an increase in $^{87}Sr/^{86}Sr$ ratios of these rocks (Şen, 2007) and, thus, a decrease in $^{87}Sr/^{86}Sr$ values of hydrothermal fluids of a marine origin. The upward movement of these fluids with diminished $^{87}Sr/^{86}Sr$ ratios in the dolomites caused recrystallization of Rd1a and Rd3 dolomites, which led to a decrease in their $^{87}Sr/^{86}Sr$. $^{87}Sr/^{86}Sr$ values of Cd dolomite are consistent with those of Rd1a and Rd3 dolomites (Fig. 7A; Table 1), which is a result of deposition of Cd dolomite by hydrothermal fluids of a marine origin that recrystallized the Rd1a and Rd3 dolomites.

5.1.4. Sr concentrations

In the studied section, dolomites of the Berdiga Formation are represented by Sr contents with a bimodal composition (Fig. 4D; Table 1). Rd1b and Rd2 dolomites (74–99 ppm, n = 10) comprising the first population have lower Sr contents than Rd1a and Rd3 dolomites (107–163 ppm, n = 13) of the second population. Sr contents of Cd dolomite ranging from 106 to 201 ppm (average 134 ppm, n = 5) are conformable with those of Rd1a and Rd3 dolomites. The average molar Sr^{2+}/Ca^{2+} ratios of solutions that formed Rd1a, Rd1b, Rd2, and Rd3 dolomites are 0.0094–0.0157, 0.0064–0.0107, 0.0052–0.0104, and 0.0097–0.0161, respectively. The molar Sr^{2+}/Ca^{2+} ratios of dolomitizing fluids computed for Rd1b and Rd2 dolomites are consistent with those of modern seawater (0,0086, Drever, 1997; D_{sr} = 0.015–0.025), but those calculated for Rd1a and Rd3 dolomites are slightly higher than seawater value. This might indicate that Rd1b and Rd2 dolomites still preserve the signals of marine origin, whereas Rd1a and Rd3 dolomites are once again recrystallized by marine hydrothermal fluids that were partly modified by mafic volcanic rocks of Şenköy Formation. In addition, recrystallization of replacement dolomites during

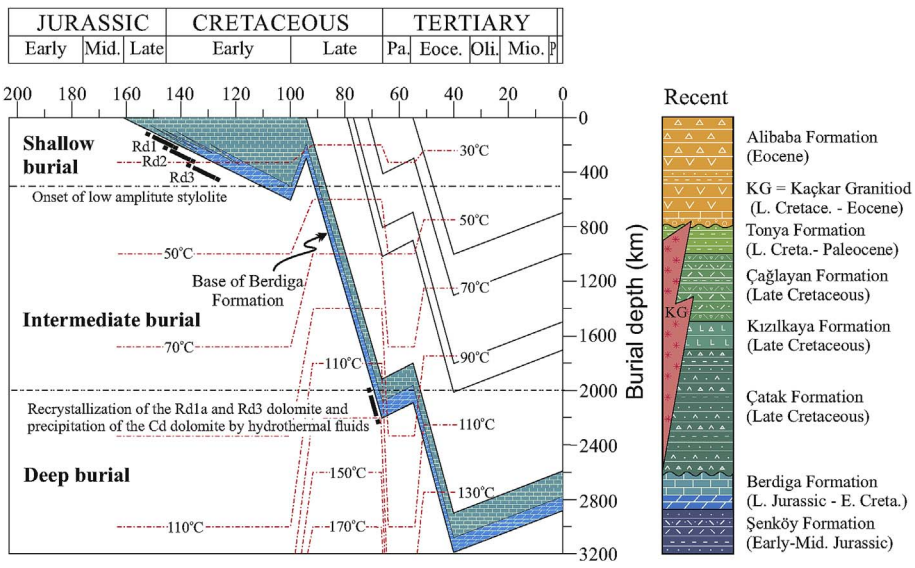

Fig. 8. Burial-temperature-time plot for the Berdiga Formation, constructed assuming a surface temperature of average 20 °C and a geothermal gradient of 30 °C $km^{-1}$and 45 °C $km^{-1}$for Late Jurassic-Early Cretaceous and Late Cretaceous, respectively. The curve is constructed using the method proposed by Lopatin (1971) and Waples (1985). Intermediate burial represents the onset of low amplitude stylolites (> 500 m; Lind, 1993), and shallow and deep burial define pre-and post-incipient stylolitization corresponding to depths of < 500 m and > 2000 m, respectively. See text for detailed explanations.

continuing burial and increasing temperature results in a decrease in their Sr^{2+} contents, whereas recrystallization of Rd1a and Rd3 dolomites by marine hydrothermal fluids leads to an additional increase in Sr^{2+} contents. The fact that Sr^{2+} contents of Cd dolomite and Sr^{2+}/Ca^{2+} ratios of fluids forming Cd dolomite are similar to those of Rd1a and Rd3 dolomites is another evidence for Cd dolomite being deposited from hydrothermal fluids of a marine origin that recrystallized Rd1a and Rd3 dolomites.

5.1.5. Na concentrations

The fact that very little is known about the sodium distribution coefficient of dolomite ($D_{Na}^{dolomite}$), which is estimated at about 2×10^{-5} (Land, 1980; Tucker and Wright, 1992; Budd, 1997) and during diagenesis it being more mobile than Sr (Veizer, 1983), makes the analytical assessment based on Na concentrations unreliable. It is also suggested that early diagenetic dolomites have higher Na contents than late diagenetic dolomites (Brand and Veizer, 1980; Land, 1980).

Na concentrations of replacement dolomites are less than 200 ppm, and they show a bimodal distribution (Table 1). Na concentrations of Rd1b and Rd2 dolomites (100–200 ppm) are consistent with those deposited from normal seawater (about 110–160 ppm) (Veizer, 1983; Qing and Mountjoy, 1988). This indicates that Rd1b and Rd2 dolomites are derived from normal seawater. Except for a few samples, Na concentrations of Rd1a and Rd3 dolomites are below detection limit (< 100 ppm) (Table 1), which is attributed to their recrystallization by Na-depleted hydrothermal fluids of a marine origin. Likewise, volcanic rocks of Şenköy Formation that are conformably overlain with Berdiga dolomites are altered by sea water (Şen, 2007); as a consequence of this interaction, these dolomitiziting fluids become Na-depleted. The upward movement of these waters into the dolomites and the subsequent recrystallization of Rd1a and Rd3 dolomites resulted in a decrease of the Na content of these dolomites (> 100 ppm). Because the Na concentrations in the whole Cd dolomite are below detection limit, it is difficult to interpret the evolution of Na history in this rock. These low Na concentrations of Cd dolomite are a result of its deposition from Na-depleted hydrothermal fluids of a marine origin that recrystallizated Rd1a and Rd3 dolomites.

5.1.6. Fe and Mn concentrations

Fe and Mn contents of dolomites yield important information on redox conditions of dolomitizing fluids and/or Fe-Mn availability rather than ionic composition of these fluids (Budd, 1997). Since distribution coefficients of Fe and Mn are larger than 1, they have relatively high concentrations in dolomites (Kretz, 1982; Veizer, 1983; Land, 1980; Morse and Bender, 1990; Vahrenkamp and Swart, 1990). Fe and Mn equilibrium concentrations of dolomites precipitating from seawater are about 3–50 ppm and 1 ppm, respectively (Veizer, 1983). However, the concentrations of these elements in dolomites that are believed to be deposited from seawater are generally reported to be much higher (Budd, 1997; Vahrenkamp and Swart, 1990). Favoring of Fe-Mn availability by reducing conditions within burial fluids (also higher levels of Fe and Mn in solution) requires that later burial dolomites have much higher Fe and Mn contents than near-surface dolomites (Warren, 2000).

In the studied section, Fe and Mn concentrations of Berdiga dolomites are significantly greater than those of dolomites deposited from normal seawater. This indicates the presence of a significant Fe and Mn source and that pore waters are of a reducing nature. As evident in the low concentrations of Fe (< 100 ppm) and Mn (8–15 ppm) of three belemnite samples (Table 1), seawater and derivatives are significantly depleted in Fe and Mn, indicating that sea water could not be the source of these elements (Veizer, 1983; Aharon et al., 1987; Fouke, 1994). The mafic volcanic-volcanoclastic rocks of the Early Jurassic Şenköy Formation that are conformably overlain by the Berdiga dolomites seem to be the most plausible source of Fe and Mn in dolomites of the Berdiga Formation. Hydrothermal alteration of ferro-magnesian minerals in these rocks may provide necessary Fe and Mn for dolomites. Recrystallization of Rd1a and Rd3 dolomites by hydrothermal fluids of a marine origin that deposited Cd dolomite caused them to have a much higher and wider range of Fe and Mn contents than Rd1b and Rd2 dolomites (Fig. 4E and F).

5.2. Interpretation of dolomitization

In the studied section, the lower part of the Late Jurassic–Early Cretaceous Berdiga Formation (nearly the 120 m part) has been pervasively dolomitized (Fig. 2). Although the mechanism of dolomitization is not exactly known, any model that helps to explain the origin of dolomites should involve some matters such as (1) a supply of Mg^{2+} and CO_3^{2-}, and (2) driven mechanisms (Zhao and Jones, 2012a, b). The proposed model should also elucidate pervasive distribution, time of formation of dolomites, and the relationship between dolomitization and diagenetic fluids (Kırmacı, 2008).

In the Berdiga Formation, the cutting of replacement dolomites (Rd) by low-amplitude stylolites may indicate that these dolomites were formed at shallow burial depths before the stylolite formation (Kırmacı, 2008). The similar textural properties of Rd1 dolomite and basinal dolomudstones (boundaries between small-sized crystals and planar crystals) indicate that these units are formed at low temperatures and during the early stages of diagenesis (Gregg and Sibley, 1984; Sibley and Gregg, 1987; Durocher and Al-Aasm, 1997; Mresah, 1998; Gregg et al., 2001; and many others).

Compaction of micritic layers with increasing burial results in porosity and permeability decrease and the formation of a well-indurated rock. In this respect, pervasive dolomitization of micritic layers can only be possible during the early stages of diagenesis (shallow subsurface), at which point dolomitizing fluids freely circulate within the layers that have a high porosity and permeability (Mresah, 1998). Machel and Anderson (1989) stated that preferential dolomitization of mud and micrite with respect to clastic carbonate deposits and calcite cement occurs as a result of the fact that they have high reactive surface areas, high porosity and permeability, and a primary unstable mineralogy (Mg-calcite and aragonite). In addition, the presence of catalysts such as clay minerals and organic compounds within mud and the micritic matrix may contribute to dolomitization. Unlike Rd1 and Rd3 dolomites, Rd2 dolomite was developed as possessing a fabric-preserving nature and in a structure wherein the primary fabric of the precursor rock was well preserved (Fig. 10). As in the case of dolomites of the Berdiga Formation, the coexistence of fabric-preserving and fabric-destructive textures is a common phenomenon in many dolomites but the origin of such textures is still controversial (Lee and Friedman, 1978; Budd, 1997; Wheler et al., 1999; Jones, 2005, 2007; Suzuki et al., 2006a,b; Zhao and Jones, 2012a). The protection of primary textures is reported to be associated with: (1) these rocks not being significantly compacted and/or not cemented before dolomitization, (2) availability of core sites in precursor limestone, (3) mineralogy of precursor limestone, and/or (4) chemical composition of dolomitizing fluids (Sibley, 1982; Sibley et al., 1994).

High-Mg calcitic and aragonitic components are preferentially dolomitized with respect to low-Mg calcite (Mresah, 1998). In these dolomites, primary textures of low-Mg calcitic components completely disappear whereas those of high-Mg calcitic and aragonitic components are well preserved (Land and Epstein, 1970; Sibley, 1982; Budd, 1997). It is clear that mimetic textures apparently will not be preserved if dolomitization occurs after high-Mg calcitic and aragonitic components are transformed into low-Mg calcitic components. This indicates that fabric-preserving Rd2 dolomite formed during early burial before aragonit and/or high-Mg calcite are stabilized to low-Mg calcite (Goodell and Garman, 1969; Wanles, 1979). Based on these data, any model proposed to explain the occurrence of Rd1 and Rd2 dolomites should be able to express their early diagenetic origin.

In the studied section, the absence of evaporite minerals in the

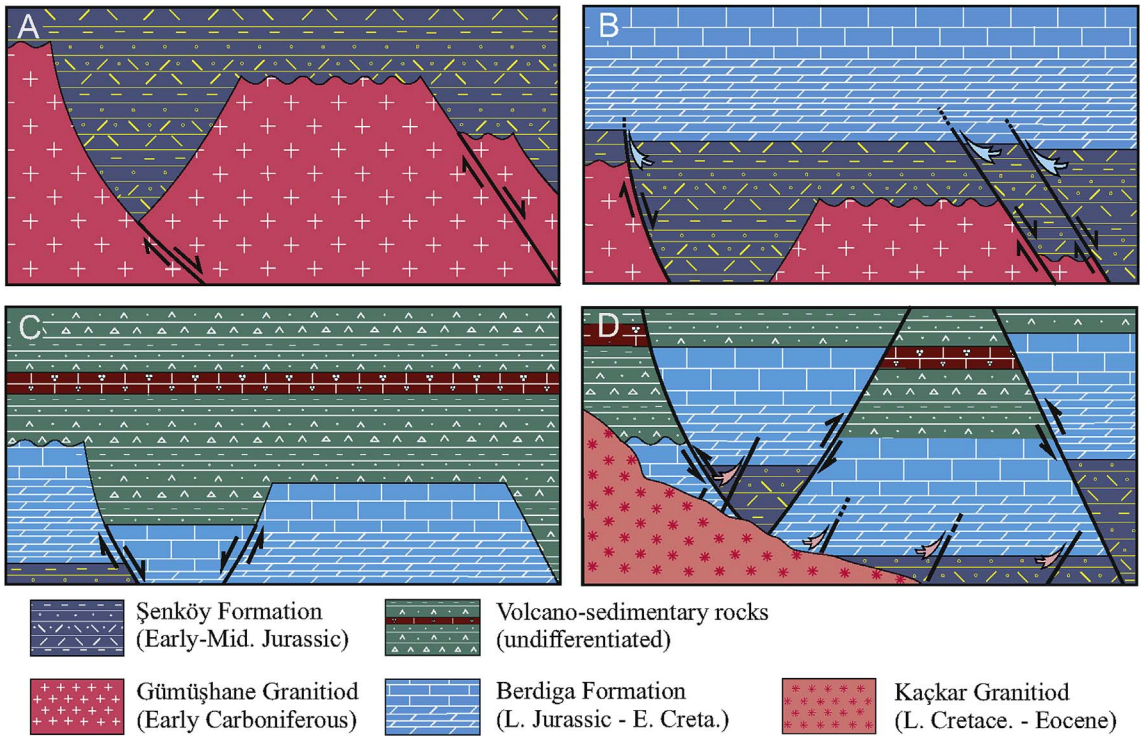

Fig. 9. Mesozoic tectono-sedimentary evolution of northern zone of Eastern Pontides (NE, Turkey). A. Rifting of pre-Jurassic basement units (granitic and metamorphic rocks). Deposition of rift basin sediments (epiclastic and pyroclastic rocks) and bimodal volcanism (Early–Middle JurassicŞenköy Formation). B. After pausing of tectonic movements and magmatism transformation of region to a carbonate platform and deposition of platformcarbonates (Berdiga Formation). Formation of replacement dolomites (Rd) at shallow burial depths (Late Jurassic–Early Cretaceous). C. Breaking of carbonate platform in association with extensional tectonic movements, formation of clastic and volcanic sequences, and development of thermal subsidence and maximum flooding surface (MFS) (Middle–Early Cretaceous). D. Basin uplift in association with compressional tectonic movements, formation of volcanic and volcano-sedimentary units, and placement of arc granitoidintrusives. Recrystallization of Rd1a and Rd3 dolomites by hydrothermal waters of marine origin and precipitation of Cd dolomite (Late Cretaceous; see text for details).

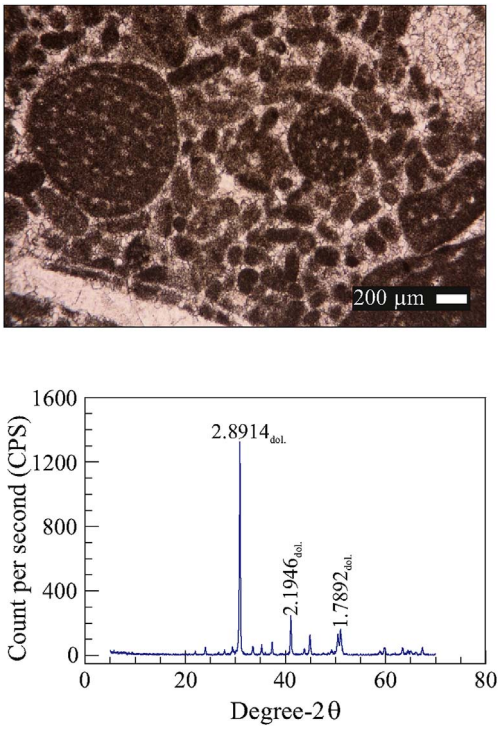

Fig. 10. A. Photomicrograph of completely dolomitized grainstone with fabric-preserving dolomite (Rd2). Note the well preserved *Favreniaesalavensis* and peloids, and B. X-Ray diffraction pattern of the same sample.

Berdiga Formation and the fact that precursor limestone that is replaced by Rd2 dolomite is composed of grainstone (Figs. 3C and 9) yield that the hypersaline sabkha dolomitization model is not effective for the formation of Rd1 and Rd2 dolomites. Considering mass-balance conditions, it is probable that only seawater and/or seawater slightly modified could supply the necessary Mg for pervasive dolomitization of carbonate rocks during early diagenesis (Land, 1980; Given and Wilkinson, 1987; Kaufman, 1994; Fu et al., 2006). Similar $\delta^{13}C$ and $^{87}Sr/^{86}Sr$ values of Rd1 and Rd2 dolomites and Late Jurassic–Early Cretaceous seawater may indicate that these dolomites were precipitated from marine waters.

Rd3 dolomite is planar-s textured and coarse to very coarse crystalline, and it has a fabric-destructive nature (Fig. 3). This yields that Rd3 dolomite was formed after stabilization of high-Mg calcitic components from fluids that are less saturated with respect to dolomite than dolomitizing fluids that crystallize the texture-protective dolomites (Sibley, 1982; Sibley and Gregg, 1987; Zempolich and Baker, 1993). Thus, Rd3 dolomite was formed before low-amplitude stylolites but after Rd1 and Rd2 dolomites. Although seawater dolomitization explains the origin of early matrix dolomite, seawater and/or seawater slightly modified due to rock-seawater interaction seems to be the most plausible source for Mg supply that is necessary for the precipitation of Rd3 dolomite. According to Machel and Anderson (1989), this type of fluid may be expelled during the mechanical compaction at an average temperature of 40–50 °C and a burial depth of 300–1000 m (using a geothermal gradient of average 33 °C km^{-1}). Such expelling of Mg-rich fluids during mechanical compaction is believed to be the main mechanism that is responsible for dolomitization and for migration of fluids from intermediate to shallow burial depths (Mattes and Mountjoy, 1980; Land, 1980; Baker and Burns, 1985; Machel and Mountjoy, 1986; Machel and Anderson, 1989; Amthor et al., 1993;

Mountjoy and Amthor, 1994). It is probable that Mg that is necessary for the deposition of Rd3 dolomite is derived from formation waters that are expelled as a result of mechanical compaction of thick shale-mudstone layers of rift basin deposits and migrates upward into the Berdiga Formation along fault and/or fracture lines bordering the basin (Fig. 8B).

A burial depth of 500 m based on a surface temperature of 16–27 °C and a geothermic gradient of 30 °C km^{-1} where low-amplitude stylolites start to form corresponds to a burial temperature of 31–42 °C (Fig. 8). The minimum formation temperatures calculated from $\delta^{18}O$ values of Rd1a, Rd1b, Rd2, and Rd3 dolomites are 88, 56, 50, and 79 °C, respectively (Fig. 5B), which, under the same geothermic gradient, correspond to minimum burial depths of 1.71, 0.97, 0.77, and 1.73 km, respectively. However, a minimum homogenization temperature (T_h) of 170 °C for RD3 dolomite requires a burial depth greater than 4.7 km. The minimum formation temperatures estimated for Rd1b and Rd2 dolomites are slightly above the proposed temperatures. This is a result of the recrystallization of Rd1b and Rd2 dolomites in a closed system and at an elevated temperature during subsequent burial (e.g. Al-Aasm and Packard, 2000; Kırmacı and Akdağ, 2005; Kırmacı, 2008; Swart et al., 2005). Considering the burial history of the Berdiga Formation, the thickness of deposits is able to provide the necessary minimum temperature for the recrystallization of Rd1b and Rd2 dolomites (Fig. 8). However, the minimum formation temperatures that are computed for RD1a and Rd3 dolomites are not consistent with their formation conditions. The burial history of the Berdiga Formation does not support any deposit thickness to meet the minimum burial depths proposed for Rd1a and Rd3 dolomites (Fig. 8). Therefore, the minimum formation temperatures computed for Rd1a and Rd3 dolomites can only result from the hydrothermal waters that recrystallized them. Although the $\delta^{18}O$ values of these dolomites are significantly depleted, their $\delta^{13}C$ values are consistent with those of the Late Jurassic–Early Cretaceous marine waters, indicating that hydrothermal waters are of a marine origin with no sign of interaction with meteoric waters. During their upward migration, these waters altered the volcanic-volcanosedimentary rocks of the Şenköy Formation (Şen, 2007), which resulted in a partial modification of their composition. As a result of this alteration, hydrothermal fluids of a marine origin became depleted in $^{87}Sr/^{86}Sr$, Sr, and Na but enriched in Ca, Mn, and Fe.

Since Cd dolomite overlies the low-amplitude stylolites (Fig. 3C and D), it must form after the stylolites. Considering that low-amplitude stylolites may occur at depths of as much as 1000 m (Lind, 1993; Duggan et al., 2001), Cd dolomite might form at depths greater than 1000 m. The burial history of the Berdiga Formation shows that the region can attain such a depth in the Late Cretaceous period when the region gains a magmatic arc nature (Fig. 8). As mentioned earlier, a homogenization temperature of 168 °C (T_h) measured on Cd dolomite crystals requires that this dolomite is formed at minimum burial depths of 3.0–3.5 km, considering a surface temperature of 16.7–27.4 °C and under a maximum geothermic gradient of 45 °C km^{-1}, which is inconsistent with the burial history of the Berdiga Formation (Fig. 8). These data show that Cd dolomite must have been formed from hydrothermal solutions at depths less than the computed minimum burial depths. Some of the Cd dolomite crystals overlying the stylolites are coarse grained and resemble saddle dolomites. Considering that saddle dolomites may quickly precipitate at high temperatures (Radke and Mathis, 1980; Searl, 1989) and they are a common indicator of hydrothermal conditions (Davies and Smith, 2006), the model proposed for the deposition of Cd dolomite seems to be valid. Overlapping geochemical signatures of Cd dolomite and Rd1a-Rd3 dolomites (Fig. 4; Table 1) and their uniform CL images (Fig. 3) may yield that Cd dolomite was precipitated from hydrothermal fluids of a marine origin under constant physicochemical conditions.

Cd dolomite by late-stage mosaic calcite cements shows that, depending on uplift and/or fault of the basin, progressive discharges of hydrothermal waters result in dolomite-undersaturated fluids that terminate dolomitization and trigger calcite deposition.

6. Conclusions

The Late Jurassic–Early Cretaceous Berdiga Formation is composed of platform carbonates that were deposited in a wide area, varying from supratidal to fore-reef slope. In the study area (Trabzon, NE Turkey), the lower parts of platform carbonates (~120 m) are pervasively dolomitized. Field observations and petrographic and geochemical studies on dolomites reveal the following results:

1 Lateral and vertical distributions of dolomite masses in the Berdiga Formation indicate that dolomitization processes are closely associated with Mesozoic tectonic evolution of the region.
2 Dolomitization of precursor carbonates is of both fabric-preserving and fabric-destructive character and petrographically, it occurs in three different texture types: (1) fine crystalline planar-s dolomite (Rd1), (2) fabric-preserving, fine–medium crystalline planar-s dolomite (Rd2), and (3) coarse–very coarse crystalline planar-s dolomite (Rd3). A minor amount of dolomite cement (Cd) appears to either partly or completely fill the vuggy/moldic porosity and fractures in Rd1 dolomite.
3 Replacement dolomites (Rd) are cut by low-amplitude stylolites, showing that they are formed at shallow burial depths before the stylolites.
4 Although Rd1 dolomite has similar petrographic and textural properties (small crystal size and planar crystal borders) as dolomites that form under a low temperature close to shallow subsurface conditions, it shows a bimodal geochemical distribution. Rd1 dolomite comprising the first population in the lower parts of the dolomite sequence (described as Rd1a) has significantly depleted $\delta^{18}O$ and lower $^{87}Sr/^{86}Sr$ values, and Na and higher Ca, Sr, and Mn contents in comparison to Rd1 dolomite (described as Rd1b) in the upper level of the sequence. This is due to recrystallization of Rd1a dolomite by marine hydrothermal waters.
5. Fabric-preserving Rd2 dolomite having similar geochemical characteristics with RD1b dolomite was formed under a low temperature and during the relatively early stages of diagenesis from waters similar to Late Jurassic–Early Cretaceous seawater.
6. Although Rd3 dolomite is cut by low-amplitude stylolites, it is represented by considerably depleted $\delta^{18}O$, positive $\delta^{13}C$ (similar to Rd1a), and high homogenization temperatures (T_h) such as 170–210 °C. This may indicate that Rd3 dolomite, which was formed under shallow burial depths, together with Rd1a dolomite were recrystallized by hydrothermal fluids of a marine origin with a significantly depleted $\delta^{18}O$ composition.
7. Cd dolomite that overlies the stylolites is represented by a homogenization temperature (T_h) of 168–185 °C and geochemical characteristics that are similar to Rd1a and Rd3 dolomite, indicating that Cd dolomite was precipitated from hydrothermal fluids of a marine origin that recrystallized the Rd1a and Rd3 dolomite.
8 During the upward migration of hydrothermal waters that precipitated Cd dolomite and recrystallized the Rd1a and Rd3 dolomite, they hydrothermally altered the volcanic rocks of the Şenköy Formation and this resulted in a partial modification of their composition. As a result of this alteration, hydrothermal fluids of a marine origin became depleted in $^{87}Sr/^{86}Sr$, Sr, and Na but enriched in Ca, Mn, and Fe.
9 Late Cretaceous granitoid intrusions (Kaçkar Granitoid) are believed to be the best possible heat source for hydrothermal fluids of a marine origin that recrystallized the Rd1a and Rd3 dolomite and precipitated Cd dolomite. This indicates that recrystallization of Rd1a and Rd3 dolomite and deposition of Cd dolomite by hydrothermal fluids of a marine origin took place during the Late Cretaceous time.

Acknowledgements

This study was financially supported by the Scientific Research Unit of the Karadeniz Technical University under contract no 8400. The appreciation is extended to Dr. Emin Çiftçi (Istanbul Technical University) for his help for microscopic studies.

References

Aharon, P., Kolodny, Y., Sass, E., 1977. Recent hot brine dolomitization in the“ Solar Lake,” Gulf of Elat, isotopic, chemical, and mineralogical study. J. Geol. 85, 27–48.
Aharon, P., Socki, R.A., Chan, L., 1987. Dolomitization of atolls by sea water convection flow: test of a hypothesis at Niue, South Pacific. J. Geol. 95, 187–204.
Akın, H., 1979. Geologie, Magmatismus und Lagerstaettenbildung im ostpontischen Gebirge-Türkei aus der Sicht der Plattentektonik. Geol. Rundsch. 68, 253–283.
Al-Aasm, I.S., Packard, J.J., 2000. Stabilization of early-formed dolomite: a tale of divergence from two Mississippian dolomites. Sedim. Geol. 131, 97–108.
Allan, J.R., Mathews, R.K., 1982. Isotope signatures associated with early meteoric diagenesis. Sedimentology 29, 797–817.
Amthor, J.E., Mountjoy, E.W., Machel, H.G., 1993. Subsurface dolomites in Upper Devonian Leduc formation buildups, central part of Rimbey-Meadowbrook reef trend, Alberta, Canada. Bull. Can. Petroleum Geol. 41, 164–185.
Anderson, T.F., Arthur, M.A., 1983. Stable isotopes of oxygen and carbon and their application to sedimentologic and paleoenvironmental problems. In: Arthur, M.A. (Ed.), Stable Isotopes in Sedimentary Geology. 10. SEPM Short Course, pp. 1–151.
Azomani, E., Azmy, K., Blamey, N., Brand, U., Al-Aasm, I., 2013. Origin of Lower Ordovician dolomites in eastern Laurentia: controls on porosity and implications from geochemistry. Mar. Petroleum Geol. 40, 99–114.
Baker, P.A., Burns, S.J., 1985. Occurrence and formation of dolomite in organic-rich continental margin sediments. Bull. Am. Ass. Pet. Geol. 69, 1917–1930.
Banner, J.L., Kaufman, J., 1994. The isotopic record of ocean chemistry and diagenesis preserved in nonluminescent brachiopods from Mississippian carbonate rocks, Illions and Missouri. Bull. Geol. Soc. Am. 106, 1074–1082.
Bodnar, R.J., 1993. Revised equation and table for determining the freezing point depression of H_2O-NaCl solutions. Geochim. Cosmochim. Acta 57, 683–684.
Boynukalın, S., 1990. Dereli (Giresun) Baraj Yeri Ve Göl Alanının Mühendislik Jeolojisi Ve Çevre Kayaçlarının Jeomekanik Özelikleri. Ph.D. Thesis. Karadeniz Technical University, Trabzon (unpublished).
Brand, U., Veizer, J., 1980. Chemical diagenesis of a multicomponent carbonate system. 1. Trace-elements. Jour. Sedim. Pet. 50, 1219–1236.
Budd, D.A., 1997. Cenozoic dolomites of carbonate islands: their attributes and origin. Earth-Science Rev. 42, 1–47.
Burke, W.H., Denison, R.E., Hetherington, E.A., Koepnick, R.B., Nelson, H.F., Otto, J.B., 1982. Variation of seawater $^{87}Sr/^{86}Sr$ throughout Phanerozoic time. Geology 10, 516–519.
Cervato, C., 1990. Hydrothermal dolomitization of Jurassic– composed of three right-stepping segments linked Cretaceous limestones in the Southern Alps (Italy): relation by relay ramps with a pronounced dip angle, to tectonics and volcanism. Geology 18, 458–461.
Chai, L., Navrotsky, A., 1995. Energetics of calcium-rich dolomite. Geochimica Cosmochimica Acta 59, 939–944.
Coniglio, M., James, N.P., Aissaoui, D.M., 1988. Dolomitization of Miocene carbonates, Gulf of Suez, Egypt. J. Sedim. Res. 58, 100–119.
Davies, G.R., Smith Jr., L.B., 2006. Structurally controlled hydrothermal dolomite reservoir facies: An over view. AAPG Bull. 90 (11), 1641–1690.
Dawans, J.M., Swart, P.K., 1988. Textural and geochemical alternations in late cenozoic bahamian dolomites. Sedimentology 35, 385–403.
Dickson, J.A.D., 1966. Carbonate identification and genesis as revealed by stainin. J. Sedim. Pet. 36, 491–505.
Dong, S., Chen, D., Qing, H., Jiang, M., Zhou, X., 2013. In situ stable isotopic constraints on dolomitizing fluids for the hydrothermally-originated saddle dolomites at Keping, Tarim Basin. Chin. Sci. Bull. 58 (23), 2877–2882.
Drever, J.I., 1997. The Geochemistry of Natural Waters, Surface and Groundwater Environments. Englewood Cliffs, New Jersey (Prentice Hall), pp. 436.
Duggan, J.P., Mountjoy, E.W., Stasiuk, L.D., 2001. Fault-controlled dolomitization at Swan Hills Simonette oil field (Devonian), deep basin west-central Alberta, Canada. Sedimentology 48 (2), 301–323.
Dunnington, H.V., 1967. Aspects of diagenesis and shape change in stylolitic limestone reservoirs. 17th World Petroleum Congress, Mexico City, Proceedings, vol. 20. pp. 339–352.
Durocher, S., Al-Aasm, I.S., 1997. Dolomitization and neomorphism of mississippian (visean) upper debolt formation, blueberry field, northeastern british Columbia: geologic, petrologic, and chemical evidence. AAPG Bull. 81, 954–977.
Fouke, B.W., 1994. Deposition, diagenesis, and dolomitization of neogene seroe domi formation coral reef limestones on curacao, Netherlands antilles. Natuurwetenschappelijke Stud. het Caraib. Geb. 133, 182 (Publications Foundation for Scientific Research in the Caribbean Region), Amsterdam.
Fu, Q., Qing, H., Bergman, K.M., 2006. Early dolomitization and recrystallization of carbonate in an evaporite basin: the Middle Devonian Ratner laminite in southern Saskatchewan, Canada. Jour. Geol. Soci. Lond. 163, 937–948.
Gao, G., Land, L., Folk, R.L., 1992. Meteoric modification of early dolomite and late dolomitization by basinal fluids, Upper Arbuckle Group, Slick Hills, Southwestern Oklahoma. Am. Assoc. Pet. Geol. Bull. 76, 1649–1664.
Gedik, İ., Kırmacı, M.Z., Çapkınoğlu, Ş., Özer, E., Eren, M., 1996. Geologic evolution of the eastern Pontides. In: Korkmaz, S., Akçay, M. (Eds.), Reports on 30th Year Symposium in Department of Geological Engineering. Black Sea Technical University, Trabzon, pp. 654–677 (in Turkish).
Gill, I.P., Moore Jr., C.H., Aharon, P., 1995. Evaporitic mixed-water dolomitization on St. Croix, U.S.V.I. J. Sediment. Res. 65, 591–604.
Given, R.K., Wilkinson, B.H., 1987. Dolomite abundance and stratigraphic age: constraints on rates and mechanisms of Phanerozoic dolostone formation. J. Sed. Pet. 57, 1068–1078.
Goodell, H.G., Garman, R.K., 1969. Carbonate geochemistry of Superior deep test well, Andros Island, Bahamas. Bull. Am. Ass. Pet. Geol. 53, 513–536.
Gregg, J.M., Sibley, D.F., 1984. Epigenetic dolomitization and the origin of xenotopic dolomite texture. J. Sedim. Pet. 54, 908–931.
Gregg, J.M., Shelton, K.L., Jhonson, A.W., Somerville, I.D., Wright, W.R., 2001. Dolomitization of the woulsrtian limestone (lower carboniferous) in the Irish midlands. Sedimentology 48, 745–766.
Güven, I.H., 1993. Doğu Pontidler'in 1/250.000 Ölçekli Komplikasyonu. MTA Genel Müdürlüğü, Ankara (unpublished).
Hardie, L.A., 1987. Dolomitization: a critical view of some current views. Jour. Sedim. Pet. 57, 166–183.
Hong, L., Teng, M., Xiucheng, T., Wei, Z., Guang, H., Di, X., Bing, L., Shujiao, S., Chengpeng, S., 2016. Origin of structurally controlled hydrothermal dolomite in epigenetic karst system during shallow burial: an example from Middle Permian Maokou Formation, central Sichuan Basin, SW China. Pet. explor. Dev. 43 (6), 1000–1012 2016.
James, N.P., Choquette, P.W., 1990. Limestones – the meteoric diagenetic environment. In: McIlreath, Diagenesis I.A., Morrow, D.W. (Eds.), Geoscience Canada Reprint Series. 4. pp. 35–73.
James, N.P., Bone, Y., Kyser, T.K., 1993. Shallow burial dolomitization and dedolomitization of mid-Cenozoic, cool-water, calcitic, deep-shelf limestones, southern Australia. J. Sedim. Pet. 63, 528–538.
Jones, B., 2005. Dolomite crystal architecture: genetic implications for the origin of the Tertiary dolostones of the Cayman Islands. J. Sediment. Res. 75, 177–189.
Jones, B., 2007. Inside-out dolomite. J. Sediment. Res. 77, 539–551.
Kaczmarek, S.E., Sibley, D.F., 2011. On the evolution of dolomite stoichiometry and cation order during high-temperature synthesis experiments: an alternative model for the geochemical evolution of natural dolomites. Sediment. Geol. 240, 30–40.
Kaufman, J., 1994. Numerical models of fluid flow in carbonate platforms: implications for dolomitization. J. Sediment. Res. 64, 128–139.
Kaygusuz, A., Chen, B., Aslan, Z., Siebel, W., Şen, C., 2009. U-Pb zircon SHRIMP ages, geochemical and Sr-Nd isotopic compositions of the early cretaceous I-Type sarıosman pluton, eastern Pontides, NE Turkey. Turkish J. Earth Sci. 18, 549–581.
Koch, R., Bucur, I.I., Kırmacı, M.Z., Eren, M., Taslı, K., 2008. Upper jurassic and lower cretaceous carbonate rocks of the Berdiga limestone- sedimentation on an onbound platform with volcanic and episodic siliciclastic influx. Biostratigraphy, facies and diagenesis (kırcaova, kale-gümüşhane area; NE-Turkey). Neues Jahrb. für Geol. Palaontologie 247, 23–61.
Kretz, R., 1982. A model fort he distribution of trace elements calcite and dolomite. Geochim. Cosmochim. Acta 46, 1979–1981.
Kırmacı, M.Z., 1992. Sedimentological Investigation of the Upper Jurassic-lower Cretaceous Berdiga Limestone in the Alucra-gümüşhane-bayburt Regions Eastern Pontides, NE, Turkey. Ph.D. Thesis. Karadeniz Technical University, Trabzon (unpublished) (in Turkish with English abstract).
Kırmacı, M.Z., 2008. Dolomitization of the late cretaceous-paleocene platform carbonates, gölköy (ordu), eastern Pontides, NE Turkey. Sediment. Geol. 203, 289–306.
Kırmacı, M.Z., Akdağ, K., 2005. Origin of dolomite in the late cretaceous-paleocene limestone turbidites, eastern Pontides. Turk. Sedim. Geol. 181, 39–57.
Kırmacı, M.Z., Koch, R., Bucur, J.I., 1996. An Early Cretaceous section in the Kırcaova area (Berdiga Limestone, NE-Turkey) and its correlation with platform carbonates in W-Slovenia. Facies 34, 1–22.
Land, L.S., 1980. The isotopic and trace element geochemistry of dolomite: the state of the art. In: Zenger, D.H., Dunham, J.B., Ethington, R.L. (Eds.), Concepts and Models of Dolomitization. 28. SEPM Spec. Publ., pp. 87–110.
Land, L.S., 1992. The dolomite problem: stable and radiogenetic isotopeclues. In: In: Clauer, N., Chaudhuri, S. (Eds.), Isotopic Signature of Sedimentary Records. Lecture Notes in Earth Science, vol. 43. pp. 49–68.
Land, L.S., Epstein, S., 1970. Late Pleistocene diagenesis and dolomitization, north Jamaica. Sedimentology 14, 187–200.
Lee, Y.I., Friedman, G.M., 1978. Deep-burial dolomitization in the Ordovician Ellenberger Group carbonates, west Texas and southeastern New Mexico. J. Sediment. Petrology 57, 544–577.
Lind, I.L., 1993. Stylolites in chalk from Leg, Ontong Java Plateau. In: In: Berger, W.H., Kroenk, J.W., Mayer, L.A. (Eds.), Proceeding of the Ocean Drilling Program Scientific Results, vol. 130. pp. 445–451.
Lopez-Horgue, M.A., Iriarte, E., Schro¨der, S., Fernandez- Mendiola, P.A., Caline, B., Corneyllie, H., Fre´e´mont, J., Sudrie, M., Zerti, S., 2010. Structurally controlled hydrothermal dolomites in albian carbonates of the Ase'on valley, basque cantabrian basin, northern Spain. Mar. Pet. Geol. 27, 1069–1092.
Lopatin, N.V., 1971. Temperature and geologic time as factor in coalification USGS translation. Akad. Nauk. SSR. Izv. Ser. Geol. 3, 95–106.
Machel, H.G., Anderson, J.H., 1989. Pervasive subsurface dolomitization of the nisku formation in central alberta. J. Sedim. Pet. 59, 891–911.
Machel, H.G., Mountjoy, E.W., 1986. Chemistry and environments of dolomitization–a reappraisal. Earth Sci. Rev. 23, 175–222.
MacNeil, A., Johns, B., 2003. Dolomitization of the petro castle formation (pliocene), cayman brac, british west indies. Sedim. Geol. 162, 2319–3238.

Malone, M.J., Baker, P.A., Burns, S.J., 1996. Hydrothermal dolomitization and recrystallization of dolomite breccias from the Miocene Monterey Formation, Tepuquet area, California. J. Sedim. Res. 66, 976–990.
Mattes, B.W., Mountjoy, E.W., 1980. Burial dolomitization of the upper devonian miette buildup, jasper national park, alberta. In: In: Zenger, D.H., Dunham, J.B., Ethington, R.L. (Eds.), Concepts and Models of Dolomitization 28. Soc. Econ. Paleontol. Mineral. Spec. Publ, pp. 259–297.
McArthur, J.M., Howarth, R.J., 2004. Sr-isotope stratigraphy. In: Gradstein, F., Ogg, J., Smith, A.G. (Eds.), A Geological Timescale 2004. Cambridge University Press, Cambridge, U.K, pp. 96–105.
Meyers, W.J., Lu, F.H., Zachariah, J., 1997. Dolomitization by mixed evaporative brines and freshwater, late Miocene carbonates, Nijar, Spain. J. Sedim. Pet. 67, 898–912.
Morrow, D.W., 1982. Descriptive field classification of sedimentary and diagenetic breccia fabrics in carbonate rocks. Bull. Can. Pet. Geol. 30, 227–229.
Morrow, D.W., 1998. Regional subsurface dolomitization: models and constraints. Geosci. Can. 25, 57–70.
Morse, J.W., Bender, M.L., 1990. Partition coefficients in calcite: examination of factors influencing the validity of experimental results and their application to natural systems. Chem. Geol. 82, 265–277.
Mountjoy, E.W., Amthor, J.E., 1994. Has burial dolomitization come of age? Some answer from the Western Canada Sedimentary Basin. In: In: Purser, B., Tucker, M., Zenger, D. (Eds.), Dolomites. A Volume in Honour of Dolomieu 21. Int. Assoc. Sedimento. Spec. Publ., pp. 203–229.
Mountjoy, E.W., Machel, H.G., Green, D., Duggan, J., Williams-Jones, A.E., 1999. Devonian matrix dolomites and deep burial carbonate cements: a comparison between the Rimbey-Meadowbrook reef trend and the deep basin of west-central Alberta. Bull. Can. Pet. Geol. 4, 487–509.
Mresah, M.H., 1998. The massive dolomitization of platformal and basinal sequences: proposed models from the Paleocene, Northeast Sirte Basin, Libya. Sediment. Geol. 116, 199–226.
Nader, F.H., Dumont, C., Shah, M.M., Garcı´a, D., Swennen, R., Daniel, J.M., Lerat, O., Doligez, B., 2009. From field study to numerical modeling of hydrothermal dolomitization in Early Cretaceous platform carbonates (Cantabrian mountains, northern Spain). J. Geochem. Explor. 101, 73.
Nader, F.H., López-Horgue, M.A., Shah, M.M., Dewit, J., Garcia, D., Swennen, R., et al., 2012. The Ranero hydrothermal dolomites (Albian, Karrantza Valley, northwest Spain): Implications on conceptual dolomite models. Oil Gas Sci. Technol.–Revue d'IFP Energ. Nouv. 67 (1), 9–29.
Okay, A.I., Şahintürk, Ö., 1997. Geology of the eastern Pontides. In: Robinson, A.G. (Ed.), Regional and Petroleum Geology of the Black Sea and Surrounding Region. 68. AAPG Memoir, pp. 291–311.
Pelin, S., 1977. Geology and Petroleum Possibilities of Southeastern Alucra (Giresun) Region. Karadeniz Technical University, Trabzon Publication 87 (in Turkish with English abstract).
Pretorius, W., Weis, D., Williams, G., Hanano, D., Kieffer, B., Scoates, J.S., 2006. Complete tace elemental characterization of granitoid (USGS G-2, GSP-2) reference materials by high resolution inductively coupled plasma-mass spectrometry. Geostand. Geoanalytical Res. 30 (1), 39–54.
Qing, H., 1998. Petrology and geochemistry of early-stage, fine-and medium-crystalline dolomites in the middle devonian Presqu'ile barrier at pine point, Canada. Sedimentology 45, 433–446.
Qing, H., Mountjoy, E.W., 1988. Multistage dolomitization in rainbow buildups, middle devonian keg river formation, alberta, Canada. J. Sedim. Pet. 59, 114–126.
Radke, B.M., Mathis, R.L., 1980. On the formation and occurrence of saddle dolomites. J. Sediment. Res. 50 (4), 1149–1168.
Searl, A., 1989. Saddle dolomite: a new view of its nature and origin. Mineral. Mag. 53, 547–555.
Şen, C., 2007. Jurassic volcanism in the Eastern Pontides: is it rift related or subduction related? Tur. J. Earth Sci. 16, 523–539.
Shackleton, N.J., Kennett, J.P., 1975. Paleotemperature history of the Cenozoic and the initation of Antarctic glaciation. Oxyg. carbon isotope analyses DSDP sites 277 (279), 743–755.
Shah, M., Nader, F.H., Dewit, J., Swennen, R., Garcia, D., 2010. Fault-related hydrothermal dolomites in Cretaceous carbonates (Cantabria, northern Spain): results of petrographic, geochemical and petrophysical studies. Bull. Soc. Géol. Fr. 181 (4), 391–407.
Sheppard, S.M., Schwarcz, H.P., 1970. Fractionation of carbon and oxygen isotopes and magnesium between coexisting metamorphic calcite and dolomite. Contrib. Mineral. Petrol. 26 (3), 161–198.
Shields, G.A., Carden, G.A.F., Veizer, J., Meidla, T., Rong, J., Li, R.-Y., 2003. Sr, C, and O isotope geochemistry of Ordovician brachiopods: a major isotopic event around the MiddleeLate Ordovician transition. Geochimica Cosmochimica Acta 67, 2005–2025.
Sibley, D.F., 1982. The origin of common dolomite fabrics; clues fromthe Pliocene. J. Sediment. Res. 52, 1087–1100.
Sibley, D.F., Gregg, J.M., 1987. Classification of dolomite rock texture. Jour. Sedim. Pet. 57, 967–975.
Sibley, D.F., Nordeng, S.H., Borkowski, M.L., 1994. Dolomitization kinetics of hydrothermal bombs and natural settings. J. Sedim. Res. 64, 630–637.
Smith, T.D., Dorobek, S.L., 1993. Alteration of early-formed dolomite during shallow to deep burial: mississippian Mission Canyon Formation, central to southwestern Montana. Bull. Geol. Soc. Am. 105, 1389–1399.
Suzuki, Y., Iryu, Y., Inagaki, S., Yamada, T., Aizawa, S., Budd, D.A., 2006a. Origin of atoll dolomites distinguished by geochemistry and crystal chemistry: kita-daito-jima, northern Philippine Sea. Sed. Geol. 183, 181–202.
Suzuki, Y., Iryu, Y., Inagaki, S., Yamata, T., Aizawa, S., Budd, D.A., 2006b. Origin of atol dolomites distinguished by geochemistry and crystal chemistry: kita-daito-jima, northern Philippine Sea. Sedim. Geol. 183, 181–202.
Swart, P.K., Melim, L.A., 2000. The origin of dolomites in Tertiary sediments from the margin of Great Bahama Bank. J. Sediment. Res. 70, 738–748.
Swart, P.K., Cantrell, D.L., Westphall, H., Handford, C.R., Kendall, C.G., 2005. Origin of dolomite in the Arab-D reservoir from the Ghawar field, Saudi Arabaia: evidence from petrographic and geochemical constraints. J. Sedim. Res. 75, 476–491.
Taslı, K., 1991. Stratigraphy, Paleogeography and Micropaleontology of Upper Jurassic–lower Cretaceous Carbonate Sequence in the Gümüshane and Bayburt Areas (NE Turkey). Ph.D. Thesis. Karadeniz Technical University, Trabzon (unpublished) (in Turkish with English abstract).
Taslı, K., Özer, E., Yılmaz, C., 1999. Biostratigraphic and environmental enalysis of the upper jurassic-lower cretaceous carbonate sequence in the Başoba Yayla area (trabzon, NE Turkey). Turk. Jour. Earth. Sci. 8, 125–135.
Tucker, M.E., Wright, V.P., 1992. Carbonate Sedimentology. Blackwell, Oxford, pp. 482.
Vahrenkamp, V.C., Swart, P.K., 1990. New distribution coefficient fort the incorportation of strontium into dolomite and its implications for the formation of ancient dolomites. Geology 18, 387–391.
Veizer, J., 1983. Chemical diagenesis of carbonates: theory and application of trace element technique. In: Arthur, M.A., Anderson, T.F., Kaplan, I.R., Veizer, J., Land, L.S. (Eds.), Stable Isotopes in Sedimentary Geology. Soc. Econ. Paleont. Mineral. 10 Short Course 3–1-3-100.
Wanles, H.R., 1979. Limestone response to stress: pressure solution and dolomitization. J. Sedim. Pet. 49, 437–462.
Waples, D.W., 1985. Geochemistry in Petroleum Exploration. Springer Verlag, Boston 223 pp.
Warren, J., 2000. Dolomite: occurrence, evolution and economically important associations. Earth Sci. Rev. 52, 1–81.
Wheler, C., Aharon, P., Ferrell, R.E., 1999. Successions of Late Cenozoic platform dolomites distinguished by texture, geochemistry, and crystal chemistry: Niue, South Pacific. J. Sed. Res. 69, 239–255.
Wilson, Edith Newton, Hardie, Lawrence A., Phillips, Owen M., 1990. Dolomitization front geometry, fluid flow patterns, and the origin of massive dolomite; the Triassic Latemar buildup, northern Italy. Am. J. Sci. 290 (7), 741–796.
Yılmaz, C., Kandemir, R., 2002. Şenköy Formation: Description of a New Formation. Abstract Book of 3rd Stratigraphy Workshop, Ankara, pp. 14 (In Turkish).
Yılmaz, C., Kandemir, R., 2006. Sedimentary records of the extensional tectonic regime with temporal cessation: Gümüşhane Mesozoic Basin (NE Turkey). Geol. Carpathica 57 (1), 3–13.
Zempolich, W.G., Baker, P.A., 1993. Experimental and natural mimetic dolomitization of aragonite ooids. J. Sediment. Petrology 63, 596–606.
Zhao, H., Jones, B., 2012a. Origin of "island dolostones": a case study from the cayman formation (miocene), cayman brac, british west indies. Sediment. Geol. 243–244, 191–206.
Zhao, H., Jones, B., 2012b. Genesis of fabric-destructive dolostones: a case study of the brac formation (oligocene), cayman brac, british west indies. Sediment. Geol. 267–268, 36–54.